Norwegian University
of Life Sciences

Master's Thesis 2019 60 ECTS

Faculty of Chemistry, Biotechnology and Food Sience

Spatial composition and development of biofilms from the HIAS biological phosphorus removal plant

Didrik Villard

Biotechnology – microbiology

Didrik Villard

Master's thesis

Spatial composition and development of biofilms from the HIAS biological phosphorus removal plant

Norges miljø- og biovitenskapelige universitet

Norway

August 2019

Supervisor

Knut Rudi

Abstract

Phosphorus is one of the most important components in fertilizer and is almost exclusively sourced from phosphate rock. Phosphate rock is mined at higher rate than new deposits are being formed and peak phosphorus is expected to be reached within the foreseeable future. It is therefore crucial to establish a renewable source of phosphorus. On the other hand, phosphorus equal to 20% of global demand is flushed into sewage every year and ends up in wastewater treatment plants, where it must be removed to prevent reaching rivers and lakes where large amounts of phosphorus can cause eutrophication. The most common method of phosphorus removal is chemical precipitation, which renders the resource unusable. HIAS WWTP in Hamar has developed a system called HIAS continuous biofilm process, which can potentially address both these issues. HIAS WWTP is a full-scale biological phosphorus removal plant that contain a group of microorganisms called phosphorus accumulating organisms (PAO) to effectively accumulate and collect biologically available phosphorus by moving the PAOs from anaerobic to aerobic phases. The system is totally dependent on the microbiota; however, knowledge about the composition and development of the biofilms in wastewater treatment plants is limited. A theorized model of the spatial composition of the biofilm have been created at HIAS WWTP. This study examines the composition of the biofilm during development, by investigating the composition of the different layers of the biofilm. The layers of the biofilm were extracted using mechanical stress and through quantification by quantitative PCR and metagenomic studies of the 16S rRNA gene through Illumina sequencing it was observed that contrary to the theorized model, the abundance of PAOs increased towards the inner layer of the biofilm. Furthermore, the phosphorus removal rate was surprisingly high (95%) early in the studied time period when average PAO proportion was 0.9%. Given that the theorized model needs to be revised, it is clear that knowledge about spatial composition is still very limited, and more studies are needed.

Sammendrag

Fosfor er en av de viktigste komponentene i gjødsel, og er tilnærmet utelukkende utvunnet fra fosforitt. Fosforitt blir utvunnet raskere enn nye avsetninger dannes, og det er forventet at «peak phosphorous» vil nås i nærliggende fremtid. Det er derfor essensielt å etablere en fornybar fosforkilde. På en andre siden forsvinner fosfor tilsvarende 20% av det globale behovet ut med kloakken hvert år, og ender opp i vannrenseanlegg, hvor det må fjernes for å unngå utslipp i elver eller ferskvann, hvor store mengder fosfor kan forårsake eutrofiering. Den mest utbredte metoden for å fjerne fosfor er kjemisk utfelling, som innebærer at produktet ikke kan benyttes videre. HIAS WWTP i Hamar har utviklet et system kalt HIAS kontinuerlig biofilm-prosess, som potensielt kan adressere begge disse problemstillingene. HIAS WWTP er et storskala, biologisk fosforrensingsanlegg, som består av en gruppe mikroorganismer kalt fosfor-akkumulerende organismer (PAO), for å effektivt akkumulere og samle inn biologisk tilgjengelig fosfor ved å forflytte PAO-ene mellom anaerobiske og aerobiske faser. Systemet er avhengig av mikrobiotaen, men kunnskap om komposisjonen og utviklingen av biofilmene i vannrenseanlegg er svært begrenset. En arbeidsmodell over den spatiale komposisjonen av biofilmene har blitt utviklet ved HIAS WWTP.

Dette studiet undersøker komposisjonen av biofilm under utvikling, ved å undersøke komposisjonen av de ulike lagene i biofilmene. Lagene ble ekstrahert ved bruk av mekanisk stress, og gjennom kvantifisering via kvantitativ PCR, og metagenomiske studier av 16S rRNA gjennom Illumina-sekvensering, ble det observert at i motsetning til arbeidsmodellen økte andelen inn mot det indre laget av biofilmen. Videre ble det funnet av fosforfjerningsraten var overraskende høy (95%) tidlig i tidsperioden, da den gjennomsnittlige PAO-andelen var 0.9%. Basert på at arbeidsmodellen må revdideres, blir det tydelig at dagens kunnskap om den spatiale komposisjonen i biofilmer fremdeles er svært begrenset, og at det trengs flere studier for å utvikle kunnskapen på dette området.

Acknowledgments

The work in this thesis was conducted at the Faculty Chemistry, Biotechnology and Food Sciences, at the Norwegian University of Life Sciences. Under the supervision of professor Rudi.

First, I am incredibly thankful to my supervisor, Professor Knut Rudi, for introducing me to this project and accepting me as his master student. To him, I am incredibly grateful for both, sharing his knowledge and experiences as well as always keeping the moral the high!

Thanks to Sondre Eikås at HIAS IKS for correspondence and for showing me around the amazing wastewater treatment!

I would also like to thank Inga Lena Angell. For withstanding all the dumb questions, I might have had through this thesis. You always kept pushing me in the right direction, without you, this thesis might never have reached the press.

This thesis would not be complete without thanking the other master students, at the laboratory. For keeping me company and making this year worth remembering, I am eternally grateful to all of you.

Table of contents

Abbreviation

AS	Activated sludge
dsDNA	double-stranded DNA
EBPR	Enhanced biological phosphorus removal
ESP	Extracellular polymeric substance
GAO	Glucose accumulating organisms
MBBR	Moving bed biofilm reactor
OTU	Operational taxonomic unit
PAO	Phosphor accumulating organisms
PCR	Polymerase chain reaction
Poly-P	Poly-phosphate
qPCR	Quantitative polymerase chain reaction
TE-buffer	Tris-EDTA-buffer
VFA	Short chain fatty acid
WWTP	Wastewater treatment plant

Introduction

1.1 Phosphorus as a resource

Apart from nitrogen, phosphorus is the most utilized element in artificial fertilizers, that's used worldwide in agriculture. However, as opposed to nitrogen, the phosphorus used in fertilizers are not renewably sourced as they are mined from phosphate rock deposits. According to USGS Minerals Yearbook, 27Mt of phosphate rock was extracted globally in 2018. The total global reserves are estimated to 70Gt (Jasinski, 2018). Based on the same principle as peak oil, Cordell argues that phosphate rock extraction follows a bell curve with a downward slope as a result of higher cost of production as the most accessible reserves are depleted first (Cordell et al., 2011). The proposed model indicated that peak phosphorus will be reached between 2050 and 2090. Critics of Cordell have argued that technological development is unaccounted for, and that the reserves should yield a sustained production for approximately hundred more years (Sverdrup & Ragnarsdottir, 2011). Either way, we are depleting the phosphate rock ores faster than they form, thus the phosphate rock is not renewable, and in the long term not sustainable. It is also worth mentioning that phosphate rock is not evenly distributed across the globe, with Morocco having the vast majority of the world's reserves (~71% in 2018) (Jasinski, 2018). This leaves most countries dependent on a select few nations to sustain their own food production. Regardless if the subject is seen through an environmental or a geopolitical lens, renewable sources needs to be located and utilized.

1.2 Phosphorus as a pollutant

Human phosphorus discharge into wastewater amounts to 3.7Mt phosphorus, which is equal to 20% of the global demand for fertilizers (Kok et al., 2018). Wastewater treatment plants (WWTP) has very specific concerns regarding P as an environmental pollutant. While phosphorus is necessary in fertilizers for agricultural soil, excess phosphorus may cause environmental issues. Phosphorus is the limiting factor in rivers and lakes, thus pollution may cause eutrophication. This is due to cyanobacteria being autotrophic and nitrogen fixing leaving P to be the only element to necessarily be introduced at high quantities for eutrophication to happen (Padedda et al., 2017). While runoff from agriculture is a major source for pollution, it has been estimated that between 30-50% comes from wastewater (Yang et al., 2010). An example of eutrophication in freshwater is Norway's biggest lake, Mjøsa, along which shoreline the city of Hamar. In 1970 the concentration was >10µg/L, compared to an estimated natural concentration 2-5 µg/L. (Løvik, 2009). To resolve the problems with eutrophication, WWTPs worldwide have been put under regulation limiting discharge of phosphorus, such as HIAS WWTP in Hamar, the study site for this thesis, where total discharge limit is 0.4 mg/L (Saltnes et al., 2017).

1.3 Chemical precipitation

Chemical precipitation he most common way of removing phosphorus from wastewater (Rybicki, 1998). This is only one of many examples of regulations put on WWTPs worldwide to deal with the issue of pollution. The wastewater is dosed with metal salts, such as Fe3+, Cu, Ca and Zn, to cause precipitation of metal phosphates that is removed from the WWTP through sedimentation. The resulting phosphate mineral is insoluble, as for example, if iron(II)sulphite is used the precipitated end product is vivianite (De-Bashan & Bashan, 2004). As a result, chemical precipitation renders the phosphates resources in the municipal wastewater remains non-renewable in the foreseeable future.

1.4 Enhanced biochemical phosphorus removal

Biological treatment of wastewater is most commonly processed through a method called activated sludge (AS). Where effluent sewage enters into an aerated reactor together with recycled sludge from the previous batch of sewage. The sludge is rich in bacteria that consume the nutrients in the wastewater, before everything is moved over to a sedimentation tank where the sludge sinks to the bottom of the tank, the processed wastewater is drained out, and the parts of the sludge is recycled (Gernaey et al., 2004).

To enhance phosphorus removal in an activated sludge plant, a tank with anaerobic conditions is added at the start of the plant before the wastewater is moved to the aerobic conditions (De-Bashan & Bashan, 2004). This method relies on a group of microorganisms called phosphorus accumulating organisms (PAO), which has the ability to store carbon during anaerobic conditions, in order to catabolize them in aerobic conditions to store phosphorus (Tarayre et al., 2016). By this enhanced biological phosphorus removal (EBPR), phosphorus-rich sludge can be removed from the sedimentation tank and is available for reuse, as opposed to precipitation (De-Bashan & Bashan, 2004). However, this process is not very efficient and is therefore not as commonly used as precipitation (Saltnes et al., 2017).

1.5 Hias continuous biofilm process

At HIAS WWTP a moving bed biofilm reactor (MBBR) has been developed to solve the problems of inefficiency observed in activated sludge EBPR. After a successful pilot plant, a 730 m^3 volume full-scale plant was started in May 2016 to treat municipal wastewater. Biofilms from the establishing of this full-scale plant is the study subject of the current study. (Sondre Eikås, personal communication, 28. August, 2018)

The MBBR is not dependent on recycling sludge as the bacteria grow on biofilm-carriers that float freely in the wastewater. The inlet leads the wastewater into an anaerobic phase where biofilm-carriers are stirred around in the wastewater. The second phase is an aerobic phase where air is pumped in (Fig. 1). This succession works as an EBPR by

facilitating PAOs to accumulate phosphorus (Saltnes et al., 2017). When the processed wastewater leaves the plant, the biofilm-carriers are moved over to the anaerobic phase where the accumulated phosphorus is released and can be collected and processed for fertilizer.

The plant is highly effective in phosphorus removal. At week 16 into the establishing of the full-scale, phosphorus removal reached 95% (Goa, 2018). By august 2018 the average phosphorus removal was >99%. (Sondre Eikås, personal communication, 13. August, 2019)

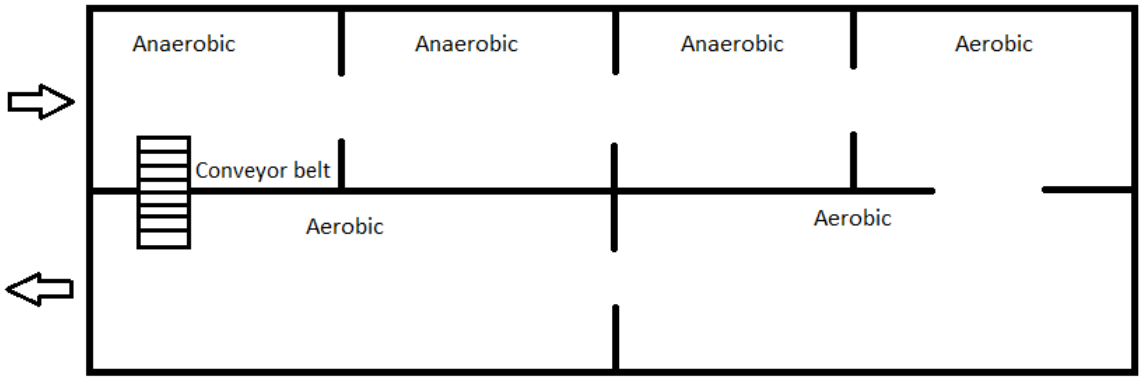

Figure 1. Schematic representation of the HIAS Continuous Biofilm Process. First, wastewater is let into the anaerobic phase. Second, wastewater flow through the plant along with the biofilms into the aerobic phase. Third, the processed wastewater leaves the plant, while the biofilms are mechanically moved into the anaerobic phase by a conveyor belt. (Saltnes et al., 2017)

1.6 Bacteria associated with biological phosphorus removal

EBPR is dependent on the microbiota for its function. While few studies have looked into composition of biofilms in WWTP, an extensive 3-year long, Danish study investigated 25 full-scale activated sludge EBPR and found a number of core species that constituted on average 80% of the microbiota in the studied plants (Nielsen et al., 2010). This suggest that the functional properties of these core species are crucial for the effectiveness of the EBPR process. The proportional distribution of these functional groups (Fig.3) is therefore of interest to the current study.

Phosphorus Accumulating Organisms

As mentioned earlier, PAOs are the microbial group responsible for the accumulation of the phosphorus, making up 13% of the average abundance of functional groups in the Danish EBPR plants, and the most abundant genus was *Accumulibacter* (Nielsen et al., 2010). *Tetrasphaera* is the second most common PAO but cannot store PHA and how their contribution to the EBPR plants works is still largely unknown (Nielsen et al., 2010).

Accumulation of phosphorus in *Accumulibacter* for EBPR is dependent on the changing between anaerobic and aerobic phases, because the stress of anaerobic conditions induces a change in metabolism (Tarayre et al., 2016). In anaerobic conditions *Accumulibacter* will use acetate, or other VFAs (Seviour et al., 2003), as a carbon source and store carbon as poly-β-hydroxyalkanoates (PHA). To convert acetate to acetyl-coA to PHA, energy is required causing the cell hydrolyse ATP into ADP. The hydrolysis releases P, which is ultimately released into the environments (Fig.2.a)

In aerobic conditions, *Accumulibacter*, catabolizes the stored PHA to acetyl-coA to use for the citric acid cycle. The released energy from the electron transport chain is used for uptake of free P into the cell, as well as to convert ADP to ATP before the ATP is used to bond the free P to a Poly-P-chain for storing (Fig.2.b)

a)

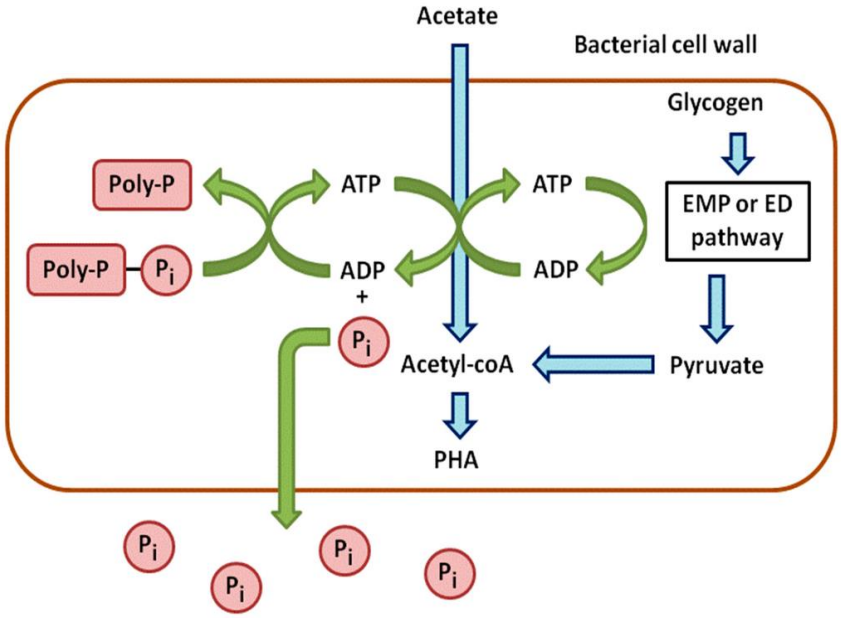

b)

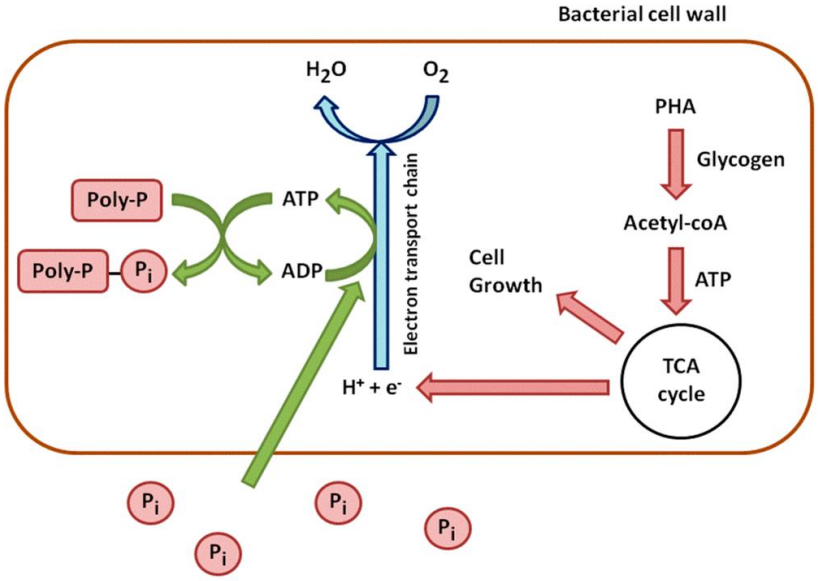

Figure 2. Metabolism of Accumulibacter. a) Anaerobic metabolism of Accumulibacter. Acetate is used as carbon source while PHA is stored. Phosphorus is released. B) Aerobic metabolism of Accumulibacter. Stored PHA is broken down and used as carbon source. Phosphorus is stored as Poly-P (Tarayre et al., 2016).

Other Functional Bacteria in Enhanced Biological Phosphorus removal

While PAOs are the desired functional group in an EBPR plant, glucose accumulating organisms (GAO) is an undesirable group which is selected for by the same selection pressures. This is because GAOs, such as *Competibacter* and *Propionvibrio*, can accumulate glucose under the same nutrient-rich and oxygen-starved conditions as the PAOs (Nielsen et al., 2010). GAOs could potentially hinder PAOs thriving by out competing them for carbon sources. However, the average abundance of GAOs found in the Danish study was considerably smaller than the PAOs, at only 1% (Fig.3).

The average abundance of denitrifiers in the Danish study was found to be 18% (Fig.3). A study has shown that some denitrifiers found in EBPR plants have the potential to use VFAs as carbon source and can therefore become a competitor to the PAOs if nitrate is available in the anaerobic phase (Baetens, 2001). This problem is eliminated at HIAS WWTP as there is no flow back as only the biofilms are moved into the anaerobic phase from the aerobic where nitrifiers produce nitrate. Furthermore, the HIAS plant has showed potential for simultaneous nitrification and denitrification (SND) during the aerobic phase (Saltnes et al., 2017).

While only making up an average abundance of 3%, fermenters is functionally important for phosphate removal, by supplying the PAOs with carbon sources, by fermenting glucose and producing VFAs (Nielsen et al., 2010). *Firmicutes* along with *Tetrasphaera* was found to be the most abundant in the Danish study.

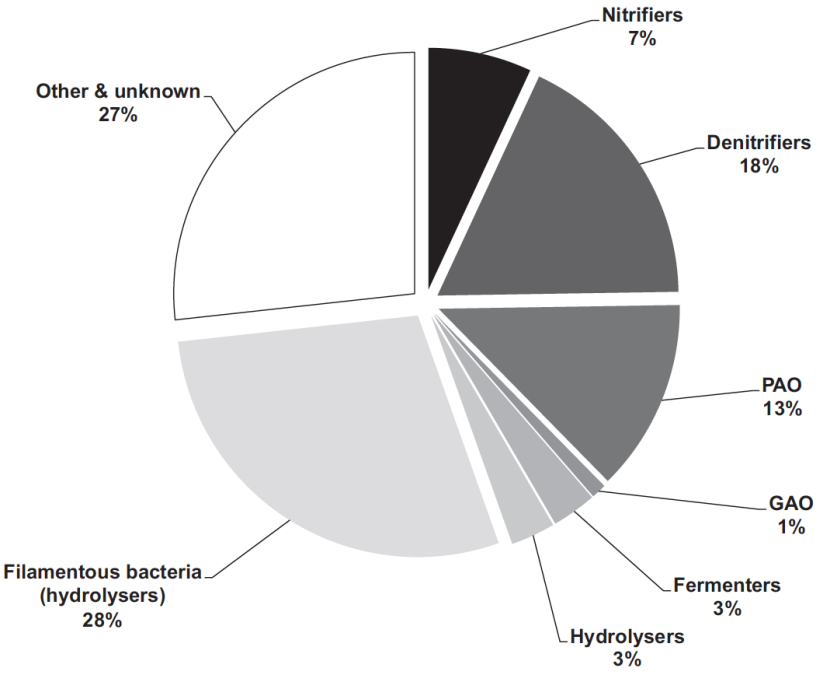

Figure 3. Average abundance of functional groups in Danish EBPR plants (Nielsen et al., 2010).

1.7 Biofilm

The way these functional groups can interact with each other is by living in close proximity encased in a biofilm, which is defined as aggregates of microorganisms in which cells are frequently embedded in a self-produced matrix of extracellular polymeric substances (EPS) that are adherent to each other and/or a surface (Flemming et al., 2016). The EPS consists of protein, DNA, lipids and other macromolecules protects the organisms living within it from the environments and it is this matrix that physically connects the bacteria in biofilm (Mahami & Adu-Gyamfi, 2011). This interconnection makes it possible for bacteria preforming different “roles” which makes it possible for specialized bacteria to thrive by dividing labor (Lappin-Scott et al., 2014). The efficiency created by the division of labor is one of many reasons why most bacteria on earth lives in biofilms and most of these biofilms are made up of multiple species (O'Toole et al., 2000).

The formation of biofilms starts with planktonic bacteria attaching a surface (Fig.4). The type of surface has been shown to make a difference in strength of attachment, where hydrophobic surfaces like plastic supporting attachment better than hydrophilic surfaces like glass (O'Toole et al., 2000). Access to nutrient is also an important factor not only during attachment, but during colonization as well, where starvation has been shown to induce dispersal (O'Toole et al., 2000). In the secondary colonization (Fig.4) nutrients have started to attach to the biofilm. When nutrients are available in the biofilm, maturation can occur, where the biofilm diversify into layers with different properties. The final stage of biofilm development is dispersal, where bacteria become planktonic and spread to form new biofilms (Mahami & Adu-Gyamfi, 2011).

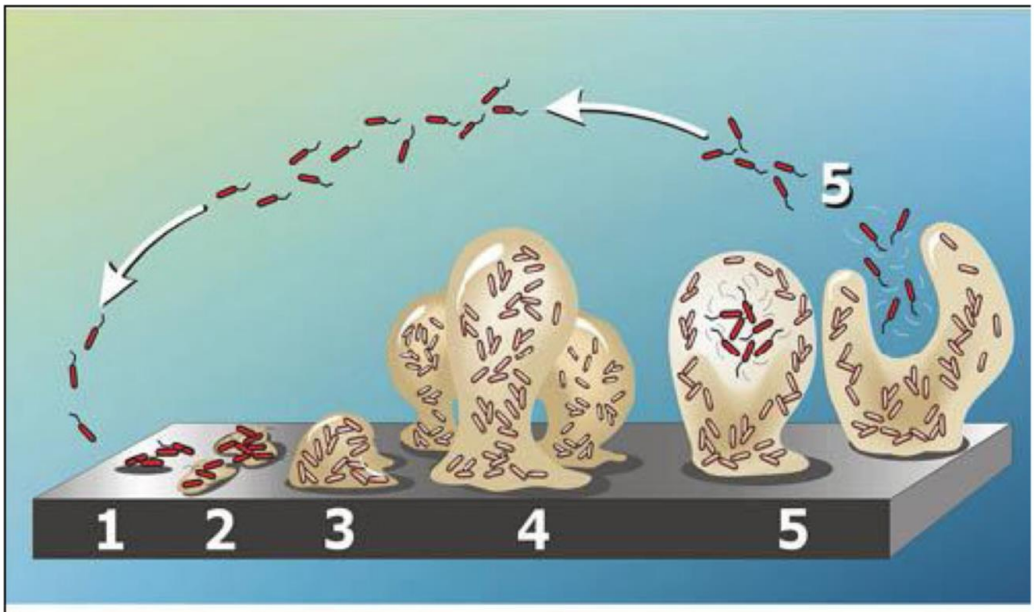

Figure 4. Biofilm development. A five stage, schematic representation of biofilm formation and development. 1) Attachment 2) colonization 3) secondary colonization 4) biofilm maturation 5) Dispersion (Mahami & Adu-Gyamfi, 2011)

Matured biofilms form complex multilayers in three-dimensional structures that support different functional groups. The layers can be loosely defined by their attachment to the biofilm, shown by the porosity range observed in mature biofilms where the outer layer was found to have a porosity of 89% and the inner layer 5% (Chmielewski et al., 2003).

Other differentiating factors include an oxygen gradient, caused by consumption of oxygen being faster than oxygen diffusion into the biofilm matrix, creating anaerobic conditions towards the inner layer, and aerobic conditions in towards the outer layer (Flemming et al., 2016).

1.8 Hias Model

Based on the theory of multi-layered biofilms a theorized model of the composition of biofilms at HIAS WWTP (Fig.5). Due to the oxygen gradient it is theorized that the inner layer of the biofilm is dominated by fermenters and anaerobic bacteria, while the middle layer where both aerobic and anaerobic conditions can arise, is where the abundance of PAOs are localized. Not pictured in the model is the theorized outer layer of loosely associated heterotrophs.

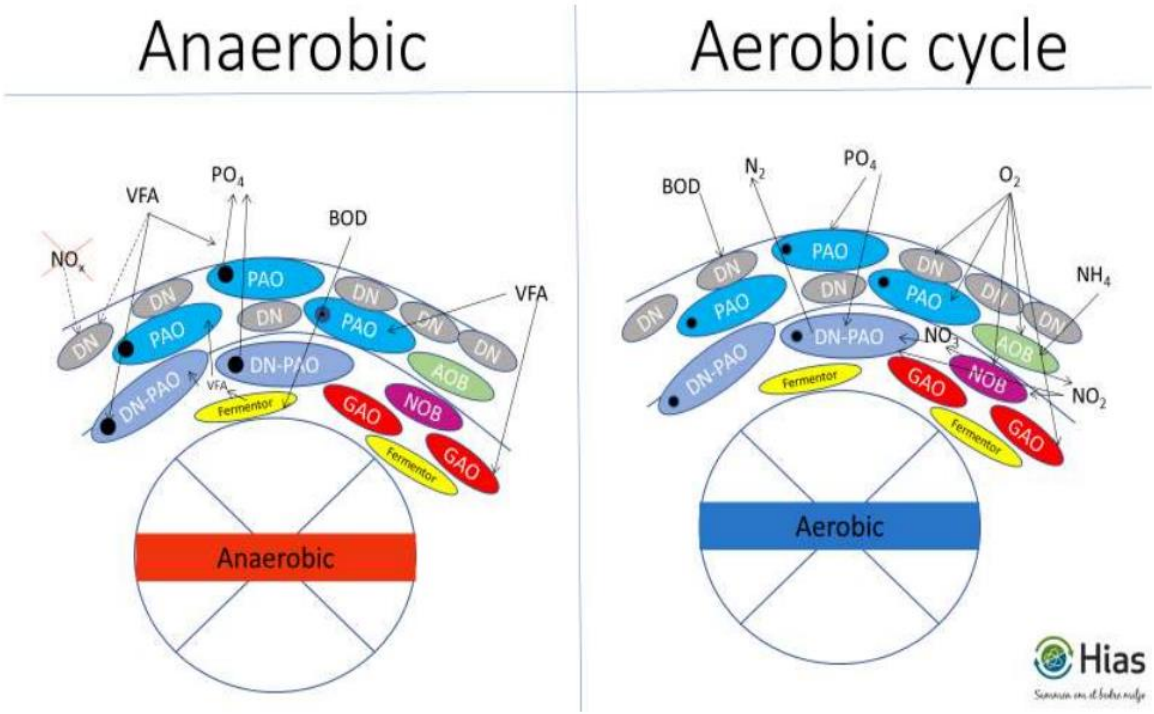

Figure 5. Theorized model of the composition of biofilms at HIAS WWTP. Fermenters and anaerobic bacteria are localized in the inner layer of the biofilm. The PAOs and denitrifiers are localized in the middle layer of the biofilm.

1.9 Fractionation

To test the theorized model of the composition of biofilms at HIAS WWTP. The current study attempts to utilize mechanical stress, a method proved to be effective to extract bacteria from biofilms (Goa, 2018), to exploit the porosity of the biofilms to extract separate layers for analysis. By gradually increasing the mechanical stress on the biofilm, different layers could potentially be extracted based on the layer's association with the biofilm. Illumina 16S rRNA metagenome sequencing will be used to determine the taxonomy and functional groups present in the extracted layers.

1.10 Aim of study

The need for renewable sources for phosphorus is expected to rise in the foreseeable future as phosphate rock deposits are diminishing. On the other hand, large quantities of phosphorus are being rendered unusable as fertilizer from WWTPs around the world in order to prevent eutrophication of rivers and lakes. Biological phosphorus removal from wastewater has the potential to address both issues. However, the efficiency of this biological wastewater treatment is highly dependent on the functional properties of the microbiota, and the composition of the biofilms in the WWTPs. The knowledge of the compositions of the microbial communities and how their interaction affects the biological phosphorus removal in the plants. Furthermore, to the authors of the present study's knowledge, there are no existing studies that examine the spatial compositions of the microbiota within the biofilms.

Therefore, the aim of this study is to determine the spatial composition during the establishment of the biofilm from HIAS WWTP.

To achieve this goal, we set the following sub-goals:

- To study the development of the biofilm in the establishing full-scale HIAS process plant.
- To study the composition of the functional groups in the biofilm.
- To study to difference in composition in the different layers of the biofilm.

Methods

2.1 Material collection

The study site for this study was HIAS WWTP in Hamar, Norway, and the material collected was K3 MBBR biofilm-carriers (Kaldnes, Norway) (Fig.6). To study the development of the biofilm in during the establishment of full-scale treatment plant, the samples were collected approximately every third week (triweekly), between 03.11.16 and 22.06.17. Triplicates from each date was selected for analysis. To optimize the fractionation and subsequent analysis of the established biofilm, the samples were collected 28.08.18 and four samples were analyzed.

All the samples were collected from the conveyor belt at the end of the aerobic zones (Fig.1) and transported on ice from HIAS WWTP, Hamar to NMBU, Ås where all samples were stored at –20^{o}C. The samples from the establishing biofilm has been thawed and refrozen since they were collected.

For the harshest treatment during fractionation of the biofilms, sand for abrasive blasting, bought at Biltema was autoclaved.

Figure 6; K3 Kaldnes biofilm-carrier. K3 has with a surface area of 500m^2/m^3 (WWF, u.å.).

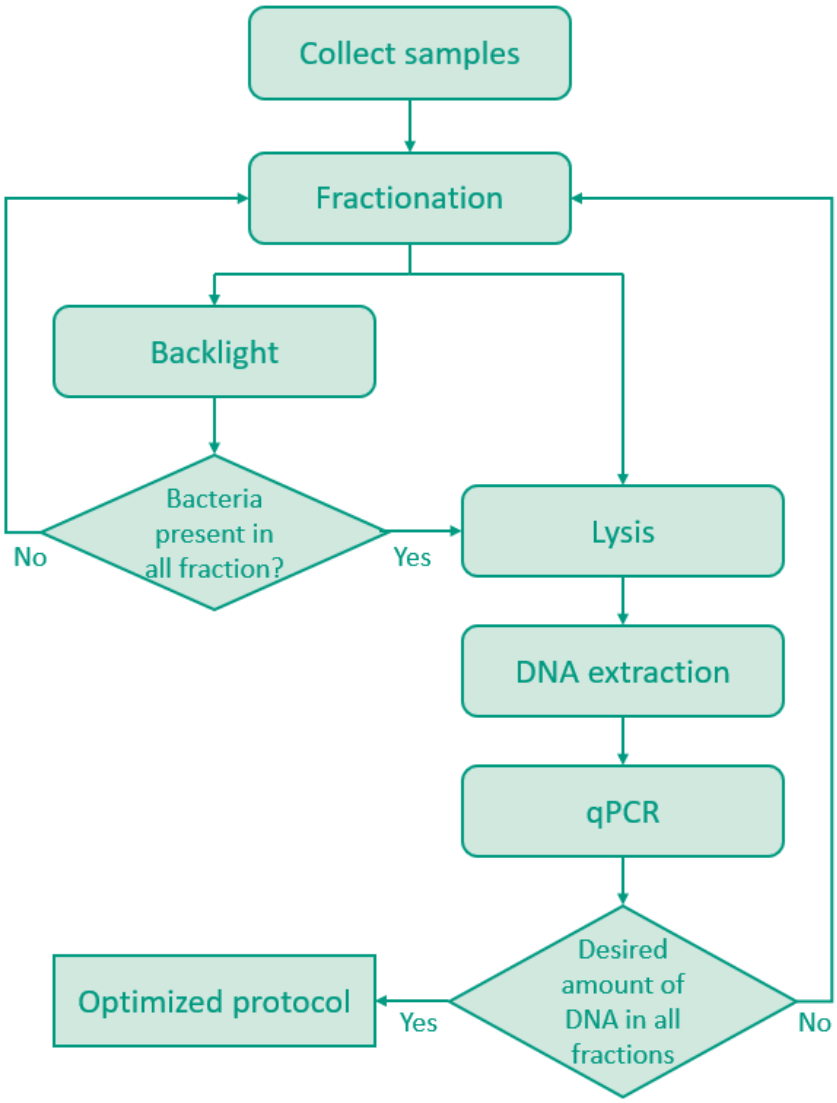

Figure 7: Flow chart of the optimization process. Material for the exploration of the fractionation strategies were collected at HIAS WWTP in Hamar, Norway. A fractionation strategy was applied, and the resulting fractions was studied under a backlight microscopy after application of LIVE/DEAD stain. If bacteria were not found in all fractions, a new fractionation strategy was applied. If bacteria were found in all fractions the bacteria samples from the fractionation step were lysed, DNA extracted from samples and quantified by a quantitative PCR. The Ct-values were analyzed and evaluated. If the set requirements for Ct-value were not met, a new fractionation strategy was applied. On the other hand, given requirements being met the tested fractionation step constitutes the optimized fraction protocol.

2.2 Optimization of the fractionation protocol

The fractionation of the biofilm into three layers based on bacteria's association with the biofilm was to be extracted by using mechanical treatment in form of shaking. To optimize the fractions, different strategies was investigated, varying the following parameters: vigorousness of shaking, time of processing, and sand, used to increase mechanical stress. Shaking was tested both on a vortex mixer and a Fast Prep 24 (MP Biomedicals, Thermo Fisher Scientific, USA) machine and vigorousness was measured in rotations per minute and meter per second, respectively. Time was measured in seconds of treatment of the aforementioned processes. Sand was added to the treatment tubes were extraction of bacteria tightly associated with the biofilm-carrier. The treatment became subsequently harsher as the previous layer was extracted with three levels of treatment, named light, medium and hard treatments. The light treatment was to be done with a vortex mixer, designed to consist of the bacteria loosely associated to the outside of the biofilm. The medium treatment was done utilizing Fast Prep 24 (MP Biomedicals, Thermo Fisher Scientific, USA) with the intent to extract the majority of the biofilm. The hard treatment included sand as a medium to loosen the bacteria that was very tightly associated with the biofilm-carrier, still using Fast Prep 24 (MP Biomedicals, Thermo Fisher Scientific, USA). Two additional fractionation steps on the Fast Prep 24(MP Biomedicals, Thermo Fisher Scientific, USA), with sand, was carried out to control that all bacteria were successfully removed.

To test how harsh the hard treatment could be without overheating the solution, tubes with a biofilm-carrier, 10mL 1:10 TE-buffer (Tris-EDTA buffer) (Sigma-Aldrich, USA) and 1,57g sand was processed at 6.5 m/s on a Fast Prep 24 at both 30 and 60 second runs with 5 min cooldown, both on and off ice in between runs.

A given fractionation strategy was tested following the protocol described in the flow chart above (Fig.7). The samples would be fractionated according to a specific setup of the given parameters and the resulting five fractions would all be stained with LIVE/DEAD stain for backlight microscopy. Staining was done, not to differentiate between live and dead bacteria, but as an initial verification that the resulting suspension contained observable bacteria. If bacteria were not observed in all the three first fractions,

fractionation strategy had to be revised. However, if backlight microscopy revealed bacterial presence in all three first fractions, then all extracted fractions would go through cell lysis before DNA extraction using a MagMidi LGC kit (LGC Genomics, UK). The extracted DNA was then quantified through qPCR. In the interest of time, the three first

fractions were ultimately going to be analyzed after a 30 cycle PCR run, therefore, these fractions had to have a Ct-value <30. Furthermore, to ensure that all detectable bacteria was extracted the 4^{th} and 5^{th} fraction had to have a Ct-value >35. If the required amount of DNA was not met, the fractionation strategy had to be revised. In the end, if each fraction was within its desired range, the optimized fractionation protocol could be used to study the establishing plant at HIAS WWTP.

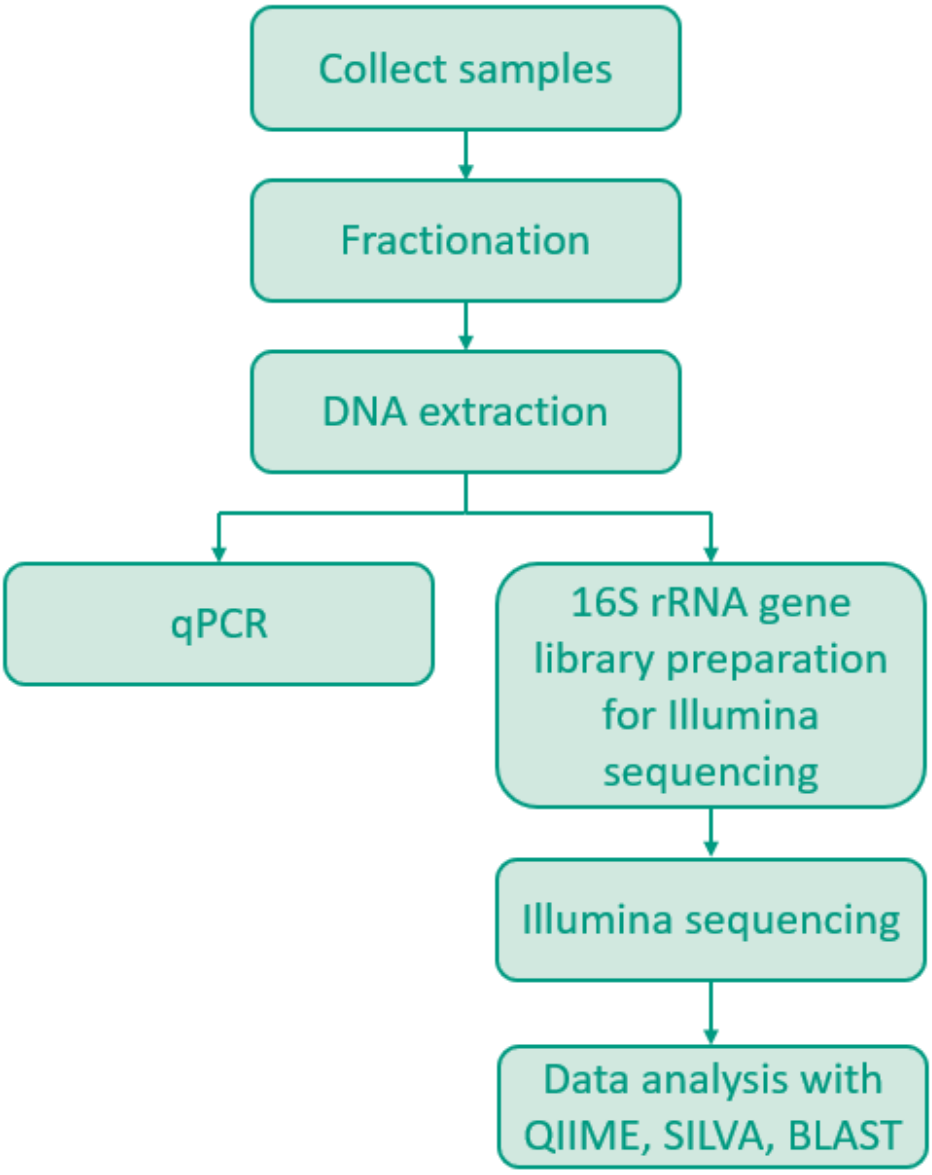

Figure 8: Flow chart of the experiments. The collected material from HIAS WWTP were fractionated using the optimized fractionation protocol. The fractionated samples were lysed, and proteinase treated before DNA was extracted. The extracted DNA from the fractionated biofilm was then both quantified by quantitative PCR and prepared for Illumina sequencing. Illumina sequencing was completed in a MiSeq (Illumina, USA). The sequences obtained were analyzed through the QIIME pipeline, reference-searched in the SILVA database. Selected OTUs were further reference-searched in the BLAST database.

2.3 The optimized fractionation protocol

The collected biofilm-carriers were thawed at room temperature, and after thawing all samples were kept on ice for all fractionation steps. All the biofilm-carriers had to stay intact to minimize unwanted mechanical stress on the biofilm, therefore tubes large enough to fit the entire biofilm. For the first fractionation step the biofilm-carrier was added to a 50mL Falcon tube (Sigma-Aldrich, USA) with 10mL 1:10 TE-buffer and vortexed on a vortex mixer for 10 sec at 3000rpm. 200µL supernatant was decanted into a FastPrep tube (MP Biomedicals, Thermo Fisher Scientific, USA) with acid-washed beads (0,2g <106um, 0,2g 425-600um, 2x 2,5-3,5mm) (Sigma-Aldrich, USA). The biofilm-carrier was carefully transferred to a new 50mL Falcon tube with 10mL 1:10 TE-buffer for the second fractionation step. The samples were processed in a FastPrep-24 on the program BG:2x50 for 60s at 6.5m/s. 200µL of the supernatant was subsequently decanted into a FastPrep tube with acid-washed beads, before the biofilm-carrier was carefully transferred to a new 50mL with approximately 1,57g sand and 1:10 TE-buffer filled to the 10mL mark. For the third fractionation step the samples were processed four times on BG:2x50 for 60sec at 6.5m/s, resting on ice for 5min between each run. After four runs 200µL of the supernatant was decanted into a a FastPrep tube (MP Biomedicals, Thermo Fisher Scientific, USA) with acid-washed beads, then the biofilm-carrier was carefully transferred into a new 50mL Falcon tube identical to the tube used for the third fractionation step. For the fourth fractionation step the samples were processed in a FastPrep-24 on the program BG:2x50 for 60sec at 6.5m/s, and 200µL of the resulting supernatant was decanted into a FastPrep tube with acid-washed beads. The biofilm-carrier was carefully transferred to a new tube identical to the one used in the third and fourth fractionation step. For the fifth fractionation step the exact same procedure as the forth fractionation step was followed, except the biofilm was not transferred to a new tube.

2.4 Isolation of DNA from the biofilm fractions

2.4.1 Mechanical lysis

To access the DNA in the bacterial cells extracted from the biofilms, mechanical lysis in FastPrep 96 (MP Biomedicals) with acid-washed beads (0,2g Sigma-Aldrich, <106um 0,2g Sigma-Aldrich, 425-600um 2x Sigma-Aldrich, 2,5-3,5mm) was administered to crush the cell walls. The TE-buffer was used instead of water to stabilize the DNA exposed to the solution after lysis. The FastPrep tubes with the fractionated samples and acid washed beads were processed in FastPrep 96 (MP Biomedicals) at 1800rpm for 40s with 5min rest between runs to prevent overheating and denaturing of the bacterial DNA. To avoid transferring the glass beads the samples were centrifuged at 13,000rpm for 5min and the supernatant was used for further extraction.

2.4.2 Proteinase treatment

Both the proteinase treatment and the DNA extraction below were performed in a KingFisher flex robot (Thermo Scientific, USA) using a MagMidi LGC kit (LGC Genomics, UK). To break down proteins and peptide bonds in the lysed samples 50µL of the supernatant of the samples in a KingFisher 96 well (Thermo Scientific, USA) plate, to which proteinase and a lysis buffer was well mixed into. The samples were then incubated at 55°C for 10min in the KingFisher flex robot.

2.4.3 DNA extraction

To extract the DNA from proteinase treated samples, paramagnetic Mag Particles were used to create salt bonds with the negatively charged DNA. Once DNA was bonded to the Mag particles, the samples were washed once with BLM 1 wash buffer and twice with BLM 2 wash buffer, to remove compounds left from the broken cells and sewage water. To release the DNA from the Mag particles an elution step was performed before the extracted DNA was stored at -20^{o}C for further analysis.

2.5 Polymerase Chain Reaction

The extracted DNA was divided into two trajectories. One was quantification through quantitative PCR, described below. The other was prepared for library of 16S rRNA gene Illumina sequencing through a two step PCR process. The first was is described under “Amplicon PCR” and was performed to amplify the 16S rRNA gene to have enough for further analysis. The second PCR process is described under “Index PCR” and was performed to attach the index primers with Illumina adapters to the PCR products from the amplicon PCR. After both of these steps were completed, the PCR products were cleaned (see “AMPure purification”) and checked on an agarose gel electrophoresis (see “Agarose Gel Electrophoresis”). All PCR protocols included a positive and a negative control, where a lab strain of *Escherichia coli* (*E. coli*) served as positive control.

2.5.1 Quantitative PCR

qPCR was preformed by mixing 0.1-10 ng/µL of DNA from samples with a final concentration of 1x “5x HOT FIREPol® EvaGreen® qPCR supermix” (Solis BioDyne, Estonia) (Appendix A.A3), 0.2uM of each the forward primer, 341F (Invitrogen™, Thermo Fischer Scientific, USA) (Appendix B.1) and the reverse primer, 806R (Invitrogen™, Thermo Fischer Scientific, USA)(Appendix B.1). The reaction mix was then amplified and quantified by a LightCycler480 II (Roche, Germany) on the following program 95^{o}C for 15min, (95^{o}C for 30s, 55^{o}C for 30s, 72^{o}C for 45s) x40.

To find the total number of 16S rRNA gene copies obtained from the fractionated samples, the Ct-values from the quantification were compared to a standard curve created by Ida Ormaasen using a lab strain of *E. coli*. The Ct-values from the standard curve was plotted against the quantity of the *E. coli* samples to generate a linear equation, which was used to calculate the common logarithm of the 16S rRNA gene copy number per sample.

2.5.2 Amplicon PCR

For the first amplicon PCR step 0.1-20 ng/µL of the DNA from the samples was mixed with a final concentration of 1x “5 x HOT FIREPol® Blend Master Mix Ready to Load” (Solis Biodyne, Estonia) and 0.2uM of each of the same primers used under “Quantitative PCR”. The reaction mix was then amplified on a 2720 Thermal Cycler (Applied Biosystem, USA) on the following program 95ºC for 15min, (95ºC for 30s, 55ºC for 30s, 72ºC for 45s) x30 (x25 for the 2nd fraction), 72ºC for 7min. The samples were kept on 4ºC for further analysis.

2.5.3 Index PCR

The index primers (Invitrogen™, Thermal Fischer Scientific, USA) (Appendix A.A.2), used for the index PCR, matched up with samples so that no samples intended for the same library had the same combination of forward and reverse primers, and dispensed into a PCR plate by a Eppendorf epMotion 5070 robot.

The reaction mix consisted of 0.1-10ng of DNA sample, 1x “5 x FIREPol® Master Mix Ready to Load” (Solis Biodyne, Estonia) (Appendix A.A.2) and 0.2uM of each of the primers. The reaction mix was then amplified on a 2720 Thermal Cycler (Applied Biosystem, USA) on the following program 95ºC for 5min, (95ºC for 30s, 55ºC for 1min, 72ºC for 45s) x10, 72ºC for 7min. The samples were kept on 4ºC for further analysis.

2.6 Next Generation Sequencing

2.6.1 16S rRNA gene metagenome sequencing

To sequence the 16S rRNA gene extracted from the fractionated biofilm, the samples had to be quantified, normalized and pooled into a library. The quantification followed the protocol described under “Quantification of PCR products with Qubit”, and the resulting concentrations was used to normalize the samples into a pooled library using a Biomek® 3000 Laboratory Automation Workstation (Beckman Coulter, USA). The resulting pooled library was purified according to the protocol described in “AMPure purification”. Subsequently, the samples were quantified in a digital droplet PCR before sequencing on a MiSeq. This part of the experiment was conducted by Inga Leena Angell.

2.6.2 Analysis of 16S rRNA Metagenome Sequencing Data

All the sequences from the samples were processed in the QIIME pipeline individually. Firstly, each sequence was processed by removing signals that had merged into one false signal, the primer sequences was removed, and a quality filter removed ambiguous sequences. Subsequently, the processed sequences were binned into OTUs based on 97% homology and the grouped sequences was systemized into an OUT-table. To discern taxonomy from the OTUs a reference-search in the SILVA database, which was added to the OUT-table. Lastly, core diversity analysis was done to produce rarefaction curves and UniFrac Principle Coordinate Analysis plots.

OTUs present >1% in any given fraction that had not been detected in the SILVA database was further analysed through a reference-search in the BLAST database. 97% homology in BLAST was used as a threshold value to for an unidentified OTU to be classified in the OUT-table.

Based on the Table of Functional groups (Appendix C) from received from HIAS WWTP, the OUT-table was divided into functional groups. The OTU-table with functional groups was used to calculate the average abundance of every functional group in every fraction in both the establishing and established biofilm. In the establishing biofilm averages were also calculated over time to give insight into development through the studied time period.

2.7 Treatment of PCR products

2.7.1 AMPure purification

Purification with paramagnetic 0.1% Sera-Mag SpeedBeads (Sigma-Aldrich, USA) was performed to remove primers, polymerases, excess nucleotides and unsuccessfully polymerized DNA strands. The discrimination of DNA strands is done by volume of beads to sample volume, where the smaller the concentration of beads only DNA strands above a certain length can bind to the beads. For the purification step performed on the amplicon PCR a 1.0x volume of beads was utilized and the process was performed on a Biomek® 3000 Laboratory Automation Workstation (Beckman Coulter, USA). However, on the pooled library a stricter selection (0.8X) was used to prevent contaminations ofprimer-dimers from the index primers. This purification was performed manually.

The 0.1% Sera-Mag SpeedBeads were brought to room temperature and thoroughly vortexed on a vortex mixer to disperse the beads evenly before gently mixed with the sample to desired concentration. The samples were incubated at room temperature for 5min, then moved onto a magnetic stand and incubated for an additional 2min for the beads to pull towards the magnet. The supernatant was carefully removed and subsequently, washed twice with 80% ethanol with each wash step incubating for 30s. After the final wash, the samples were left to dry before nuclease-free distilled water was added.

2.7.1 Agarose Gel Electrophoresis

Agarose gel electrophoresis was used to separate DNA fragments (between 100 bp-25kb) for imaging to assess if the PCR run has successfully amplified the 16S rRNA gene by visualizing bands of DNA fragments of 450-500bp.

Agarose (Sigma Aldrich, Germany) was dissolved into boiling 1x tris-acetate ethylenediaminetetraacetic acid (TAE) buffer to create a gel with 1.5% agarose. The solution was cooled down to approximately 60^{o}C before Peq (Saveen & Werner, Sweden) was added, in order to not destroy the fluorescent properties of Peq, which in a complex with DNA is detectable under UV light. The gel was poured into a mold with a comb to create wells, into which the PCR products were added to each. All samples were

measured up against a 100 bp ladder (Solis BioDyne, Estonia). The gel was put in an electrophoresis chamber and run at 85V for 35min, before the gel was into a Molecular Imager® Gel Doc™ XR Imaging system with Quantity one 1 – analysis software v.4.6.7 (BioRad, USA).

2.7.1 Quantification of PCR products with Qubit

For quantification of PCR products, Quant-iT™ was diluted 1:200 in Quant-iT™ buffer into to produce a Quant-iT™ Working Solution (Life Technologies, USA). The samples was added to the working solution at a 1:35 concentration, to make dsDNA fluorescent by binding to the fluorophores in the working solution. Detection of dsDNA in the samples were performed in a nunc plate by a Cambrex –FLX 800 CSE (Thermo Fischer Scientific, USA). However, the Cambrex can only give relative results, hence a selection of the samples together with two standards from the Qubit™ dsDNA HS Assay Kit (Thermo Fischer Scientific, USA) were quantified in a Qubit™ fluorometer (Thermo Fischer Scientific, USA). The standard curve produced from the Qubit quantification was subsequently used to calculate the absolute concentration of template DNA in the samples.

Results

3.1 Optimization of the fractionation protocol¨

The first part of the experiment was exploring different strategies of fractionating a biofilm into different layers depending on their adhesive properties. The goal was to divide the biofilm into three layers in three fractionation steps. To monitor if all detectable bacteria were extracted from the biofilm-carrier, a 4th and a 5th fractionation step was established. The theorized layers were: outer layer, consisting of the bacteria loosely to the outside of the biofilm; the middle layer, consisting of bacteria majority of the biofilm; the inner layer, designed to be consisting of the bacteria that is very tightly associated with the biofilm-carrier. The samples for the optimization of the protocol were collected 28.08.18 at HIAS WWTP, and the optimization followed the flow chart in Figure 8, results are not shown.

3.1.1 The outer layer

The first strategy tested the first fractionation step on 3s at 500rpm on a vortex mixer and resulted with a 1st fraction with a very low bacterial count found in backlight, and no qPCR data was needed. In order to establish DNA levels sufficiently high to be detected downstream, Ct-values had to be <30 to be reliably visible after a 30 cycle PCR. On the other hand, the resulting fraction was intended to constitute the outer loosely associated layer of the biofilm, hence at Ct-value <20 would be considered too low. With this in mind, three different strategies for the first fractionation step was tested: the first was 10s at 1000rpm on a vortex mixer, the second was 10s at 3000rpm on a vortex mixer, and the third was 30s at 4m/s on a Fast Prep 24. This test resulted in 10s at 3000 rpm on a vortex mixer giving the most reliable results within the desired range for the 1st fraction.

3.1.2 The middle layer

For the second fractionation step, two runs of 30 seconds of 6.5m/s on a Fast Prep 24 and revealed a large bacterial count under backlight microscopy. However, testing for temperature revealed that 60 seconds at 6.5m/s in the Fast Prep 24 twice with a 5 min cooldown with no ice overheated the sample while the sample on ice did not overheat. Therefore, in the interest of time, the same program was run once for the second fractionation (without sand) and showed similar results as two 30 second runs on the same velocity. The qPCR data showed an average Ct-value of ~18, ranging from 20.09 to 16.72, consistent with the middle layer being the majority of the biofilm.

3.1.3 The inner layer

The third fractionation step was set out to extract all remaining detectable bacteria, using sand in the buffer solution to extract bacteria tightly associated with the biofilm-carrier. All strategies for the third fractionation step used approximately 1,57g sand, and the first fractionation constituted of two runs of 30 seconds at 6.5m/s in the Fast Prep 24. To monitor bacterial extraction two additional fractionation steps were run, both on the same program as the third fractionation. Both backlight and qPCR results revealed bacteria in both 4^{th} and 5^{th} fraction, and the third fractionation step was increased to six runs of 30 seconds on 6.5m/s, while the two latter fractionation steps remained the same as described above. However, results from the revised strategy proved yet again to have detectable bacteria in both 4^{th} and 5^{th} fraction, thus the third fractionation step had to be further expanded. In addition, tests on overheating proved that time could be cut by merging two runs of 30 seconds on 6.5m/s to one run of 60 seconds on 6.5m/s if kept on ice in between runs. Therefore, the revised strategy for the third fractionation step was four runs of 60 seconds on 6.5m/s, and the fourth and fifth fractionation steps were both one run of 60 seconds on 6.5m/s each. qPCR of the last strategy revealed the 5^{th} fraction to be indistinguishable from a negative control, and it was concluded to keep the 4^{th} fraction as part of the experiment, with the fifth fractionation step being a control.

3.2 Validation of optimized protocol

To validate the method contrived from the results described above, four samples collected 28.08.18 at HIAS WWTP was fractionated, before full examination with quantitative assessment through qPCR and taxonomic analysis using Illumina sequencing, both methods on the 16S rRNA gene. The resulting four fractions proved different from each other in both size and bacterial composition, made up the described layers of the biofilm: 1st fraction makes up the outer layer, 2nd fraction makes up the middle layer, and 3rd and 4th fraction make up the inner layer. Given the revealed difference in biological makeup of the layers of the biofilm the method proved valid and the results from the validation of the optimized fractionation method constitutes the established biofilm at HIAS.

3.3 Quantification of the layers of the biofilm

qPCR of the 16S rRNA gene of the extracted DNA samples from each fraction revealed quantifiable differences in gene copy number in the different biofilm layers and were by largest to smallest: middle layer, inner layer and outer layer. Figure 9 shows the amount of copies of 16S rRNA genes in each fraction given in common logarithm. The 2nd Fraction was the largest at 6.35, the 3rd Fraction was the second largest at 5.82, followed by the 1st Fraction at 4.64 and lastly, 4th Fraction at 4.17. The 3rd Fraction therefore constitutes 86% of the inner layer by copy number of 16S rRNA gene.

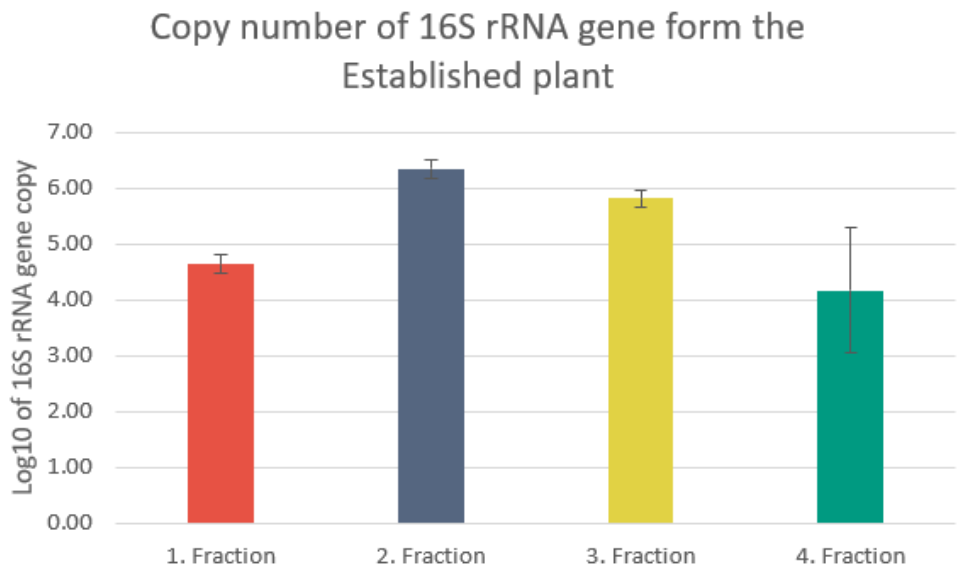

Figure 9: Quantification of the established biofilm. Common logarithm of total copy number of 16S rRNA gene from each extracted fraction from the established biofilm.

3.4 16S rRNA metagenome analysis

The microbiota from all fractions in the established biofilm were determined through 16S rRNA metagenome sequencing, where 1,090,714 sequences were obtained. These were analyzed using the QIIME pipeline and binned into OTUs based on 97% homology using the SILVA database with a cutoff at 10,000 sequences. The binned OTUs were used to construct OTU-tables and the resulting OTU-table contained 600 OTUs from the established biofilm. Sequences present in any fraction >1%, which could not be binned on a general level, were analyzed using the BLAST database, with a cutoff at 97% homology. The 5th fraction from the established biofilm did not show any resulting sequences at the 10,000-sequence cut-off.

3.4.1 Observed OTUs in the different layers

The rarefaction curves, calculated from the binned OTUs in QIIME by plotting observed OTUs against number of sequences per sample showed a difference in diversity in the different fractions. The fraction with the highest amount of DNA, the 2nd fraction, had the highest number of OTUs, while the 1st fraction had the lowest (Fig.10). The 3rd and 4th fraction were found to have the most similar alfa-diversity, with the 3rd Fraction having slightly higher diversity than the 4th fraction (Fig.10).

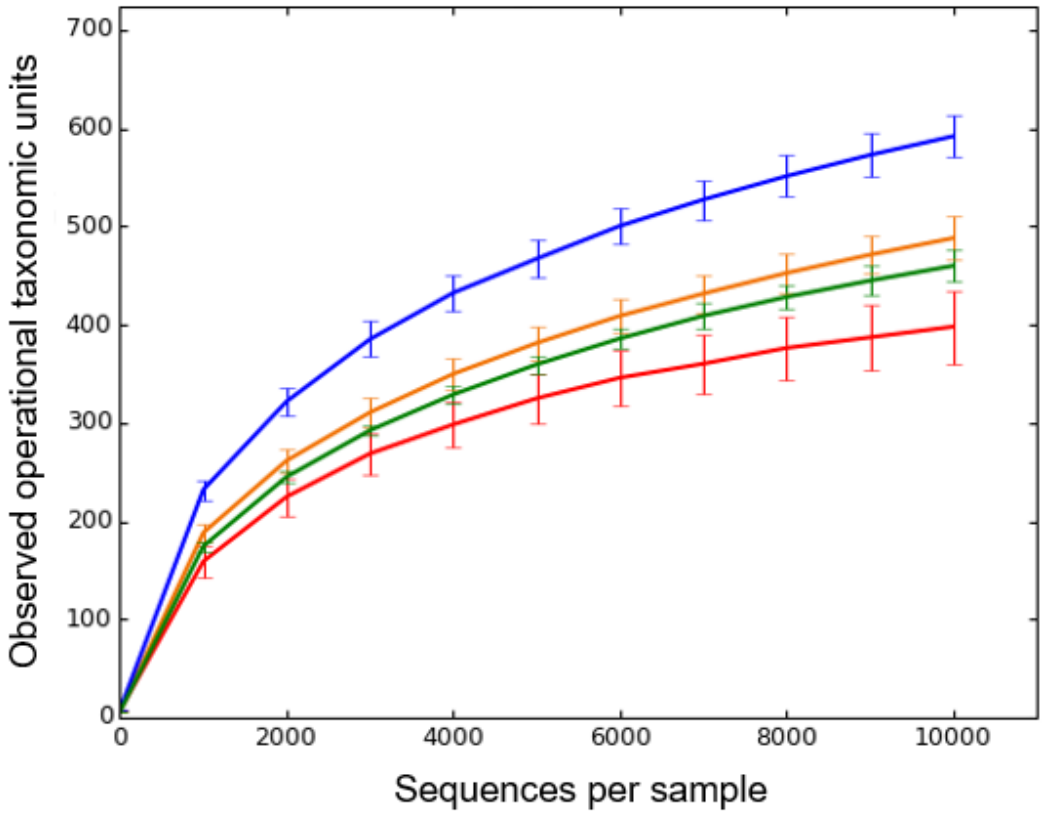

Figure 10: Observed OTUs established biofilm. Rarefaction curves of observed OTUs plotted against sequences per sample for each extracted fraction from the established biofilm. 1st fraction (red), 2nd fraction (blue), 3rd fraction (orange) and 4th fraction (green).

3.4.2 Difference in diversity between the layers

Analyzing the diversity between the fractions derived from the fractionation was performed to distinguish the fractions and to assess the validity of assigning distinct layers. Clustering of samples with unweighted UniFrac principal coordinate's analysis (PCoA) showed that the extracted layers are not only distinctly different from the other layers, but they are internally consistent between layers (Fig.11). The tightest cluster was found in the largest layer, the middle layer, suggesting that the extracted 2nd fraction has a consistent OTU composition in all samples. This was independent of the 1st fraction where the samples are had the biggest spread of any fraction in the established biofilm. However, the samples from the first fractionation step was found to have a distinct cluster in the PCoA plot and was the fraction that differentiated the most from the other extracted fractions, thus having the least overlapping OTU composition of the fractions. The only fractions to show overlap Figure 11 were 3rd and 4th, where both were found to have defined clusters distinct from the other fractions. Given their similar number of observed OTUs and their similar beta-diversity the 3rd and 4th fraction are to be considered two subdivisions of the inner layer of the biofilm.

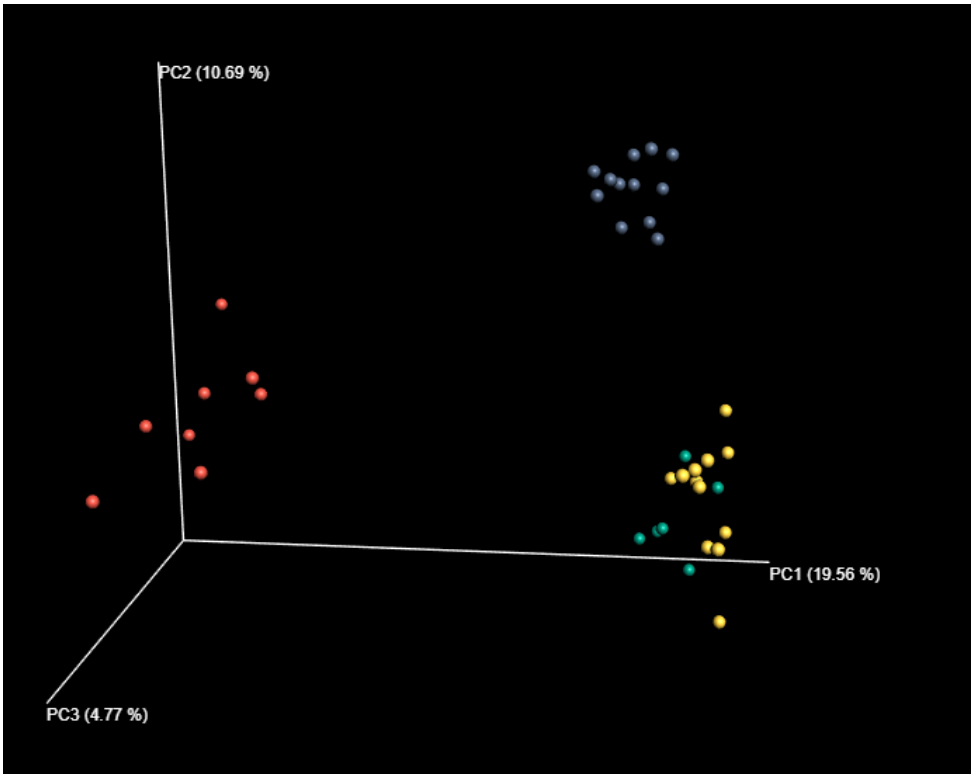

Figure 11: Beta-diversity established biofilm. Unweighted UniFrac PCoA plot showing the degree of overlap in OTU composition between the fractions of the samples collected from the established biofilm. 1st fraction (red), 2nd fraction (blue), 3rd fraction (yellow) and 4th fraction (green).

3.5 Functional groups

Categorization of all the known OTUs into functional groups revealed distinct functional differences between the layers of the biofilms, given the dissimilar proportional distribution of the functional groups.

Phosphorus accumulating organisms In the established biofilm the proportion of PAOs increases the further into the biofilm observed (Fig.12) and among the PAOs *Accumulibacter* is the most prominent genus and accounted for 95.5% of the PAOs. The most loosely associated layer, the outer layer, had the lowest proportion of PAOs at 15.8%. In the largest layer, the middle layer, a large increase from the outer layer was found at 29.7%. The largest proportion of PAOs was found in the inner layer, made up of

the 3rd and 4th fraction, which had an average proportion of 44.4%. Furthermore, the subdivision of the inner layer had a higher proportion in the fraction most tightly associated with the biofilm carrier than the larger fraction of the layer with the 4th fraction, at 48.8% and the 3rd fraction at 40.1%. The GAO proportion was slightly increasing the further into the biofilm observed, however the ratio of GAO proportion to PAO proportion was low throughout the biofilm. Only two GAOs were identified in the established biofilm, *Propionivibrio* and *Candidatus Competibacter*, in fairly equal proportions.

3.6 Other functional groups

Denitrifiers represented the second most prominent functional group in the biofilm, but the denitrifier proportion was reverse correlated with the PAOs in terms of spatial occurrence. The majority of the observed functional groups of the outer layer, 45.3%, were denitrifiers, and 62.4% of them were from the genus *Hydrogenophaga*. Denitrifers was shown to diminish further in the biofilm, as the group had a presence of 12.2% at the middle layer and 7.4% at the inner layer. Fermenters were most represented in the middle layer where the group accounted for 12.2% of the observed OTUs, where *Proteiniclasticum* was the most abundant genus making up 17.2% of the fermenters in the 2nd fraction. The inner layer had a higher abundance of fermenters than the outer layer, with a proportion of 10.0% and 5.4%, respectively. The proportion of unknown bacteria in the established biofilm was largest in the middle layer at 42.0%, followed by the inner layer at 35.1% and the smallest proportion of the unknown bacteria was found in the inner layer at 31.1%. The group with unknown functions is a diverse group, including many sequences that were unidentifiable by the SILVA database. The two identifiable genera that was most abundant of the unknown bacteria was *Delftia*, at 3.4%, and *Desulfobulbus* at 2.4%, of the average proportion in the established biofilm.

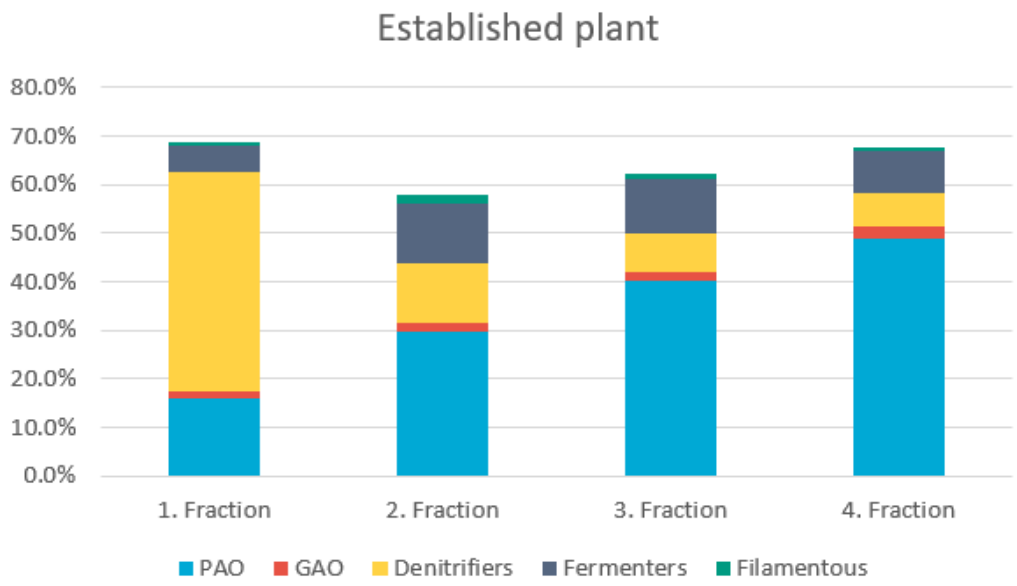

Figure 12:. Functional groups in the established biofilm based on the constructed OTU table from the QIIME pipeline. Percentage of the abundance of functional groups of bacteria from each extracted fraction from the the established biofilm, collected 28.08.18.

3.7 Results from the establishing biofilm

Fractionation and 16S rRNA gene metagenetic analysis of the triweekly samples collected at HIAS WWTP between 03.11.16 and 22.06.17 resulted in only three fractions constituting the different layers of the biofilm: the outer layer represented by the 1st fraction, the middle layer represented by the 2nd fraction, and the inner layer represented by the 3rd fraction. The fourth and fifth fractionation step only consisting of environmental contaminants found in the negative controls as well (Fig.13)

Quantification of the fractions of the biofilm over time

Quantification of the 16S rRNA gene through Real Time qPCR revealed differences in the DNA amount extracted from the different fractionation steps both over time and on average. Differences in The 2nd fraction was consistent throughout the study period and was in general the largest fraction during establishment. This fraction also corresponded well with the 2nd fraction of the established biofilm, with an average common logarithm of 6.76 over the given time period, compared to 6.35 in the established biofilm. While, the 2nd fraction was stable throughout the tested time period, the 1st and 3rd fraction fluctuate over time. These fluctuations showed some trends, such as the 3rd fraction was on average showed to contain a higher amount than the 1st fraction (exceptions being 03.11.16, 22.12.16 and 02.02.17) (Fig.13), both had in general lower amount of DNA than the 2nd fraction, and a spike of extracted DNA were observed in 1st and 3rd fraction between 24.02.17-05.04.17, in the 3rd fraction the amount observed exceeded that found in the 2nd fraction both on 15.03.17 and 05.04.17. This occurred without noticeable reduction in observed DNA amount in the 2nd fraction, proving a higher total amount of DNA extracted in the aforementioned period.

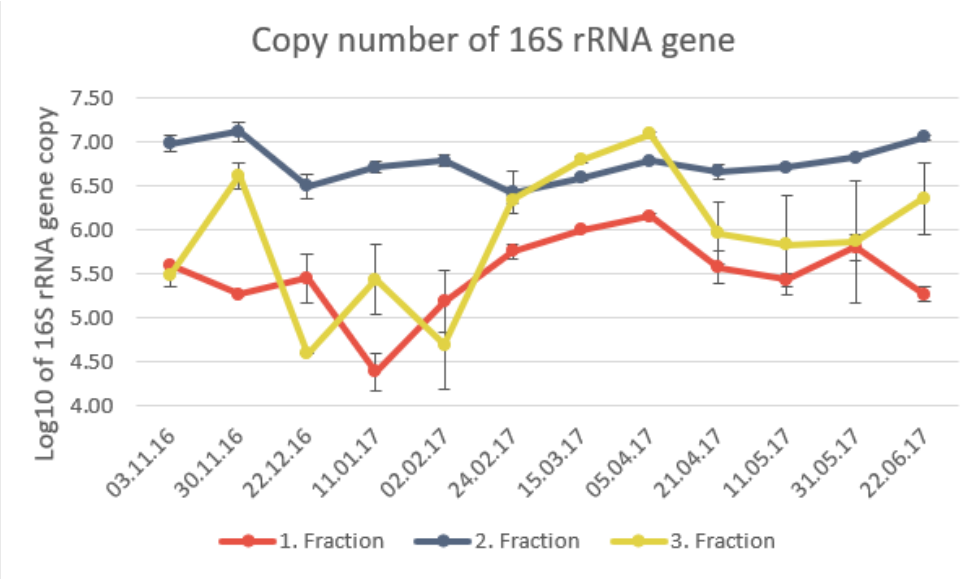

Figure 13: Common logarithm of the total copy number of 16S rRNA gene plotted against each fraction extracted from the triweekly samples from the establishing biofilm.

3.8 16S rRNA gene analysis

Two sequencing runs on the 16S rRNA gene extracted from the triweekly samples from the establishing biofilm found a total of 20,647,725 sequences, which were binned into OTU's based on 97% homology using the SILVA database after being analyzed using the QIIME pipeline. These results were used to construct an OTU table with all 889 detected OTUs. If an OTU was present at >1% in any given fraction, which had not been categorized on a genera level, the representative sequences were analyzed using the BLAST database with a cutoff at 97% homology. All the known OTU's were categorized into functional groups and the proportion of each group was calculated from the OTU-table. The proportions for each date in the establishing biofilm is the average proportion of the samples at the given date.

3.8 Observed OTUs

Rarefaction curve created by plotting the number of observed OTUs from the OTU tables against sequences per sample obtained from the establishing biofilm showed difference in the diversity of the extracted fractions. As in the established biofilm, the 2nd fraction had the highest number of OTUs in the establishing biofilm. Following the same trend, the 3rd fraction had the second highest number of OTUs. However, whereas the 4th fraction had similar OTU numbers the 3rd fraction in the established biofilm, the 4th fraction in the establishing biofilm together with the 5th fraction more similar OUT number as negative controls

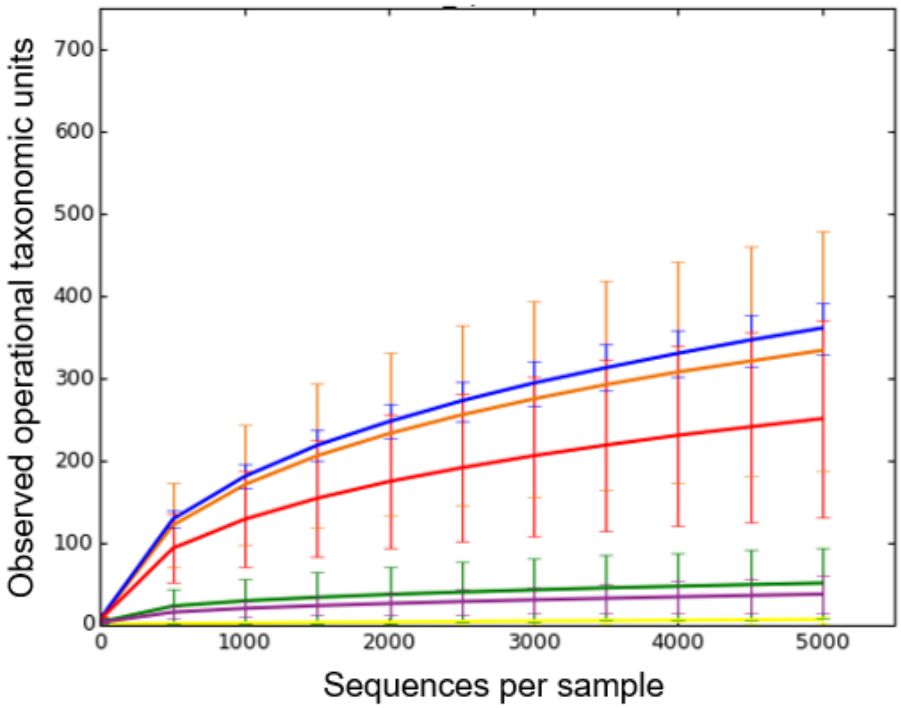

Figure 14:. Rarefaction curves of observed OTUs plotted against sequences per sample for each extracted fraction from the established biofilm. 1st fraction (red), 2nd fraction (blue), 3rd fraction (orange), 4th fraction (green), 5th fraction (purple) and negative controls (yellow).

3.9 Difference in diversity between the layers

The unweighted UniFrac principal coordinate's analysis (PCoA) used to create the plot for beta-diversity revealed the first three fractions distinctly different from each other. Even given the changes over time the samples from each fraction was found together in defined clusters (Fig.15). The 2nd fraction was the tightest cluster with no samples found outside of the cluster, while both the 1st and 3rd fraction had some samples that are not clustering with the others and with a few samples overlapping into adjacent clusters. As in the established biofilm, the 1st fraction had that largest spread within the cluster. The 4th and 5th fraction was found in the same general cluster as the negative controls and were not further studied in the taxonomic analysis.

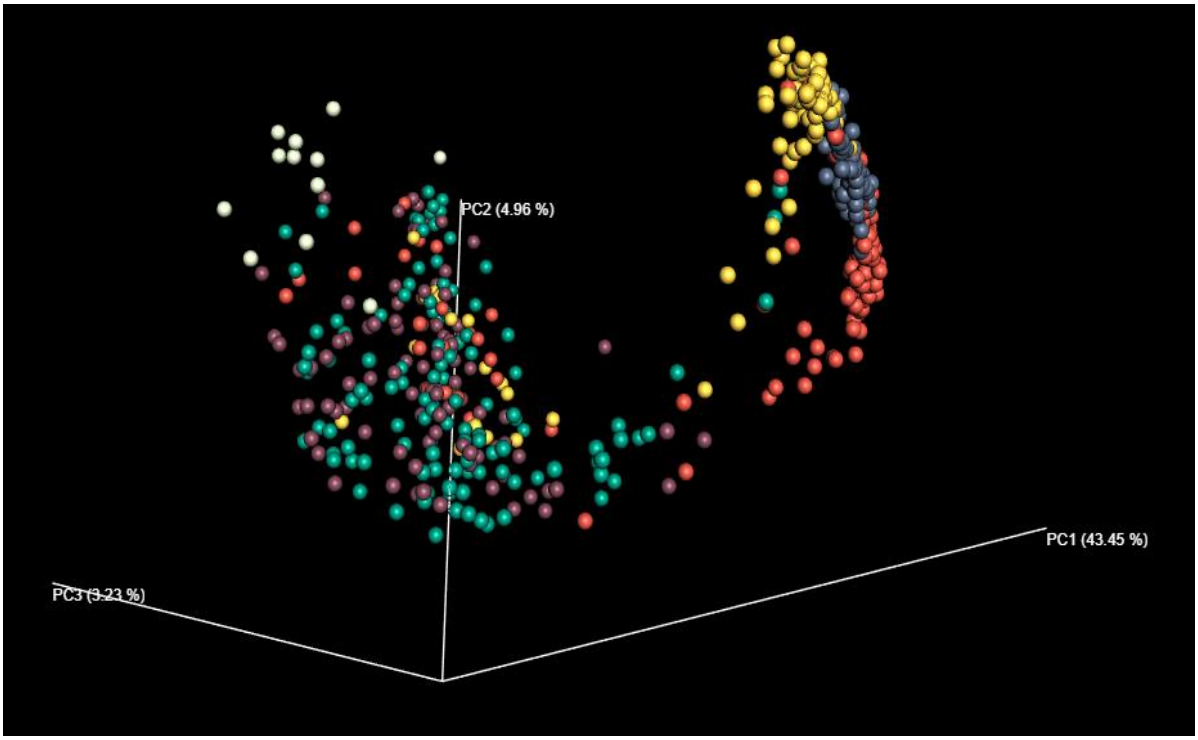

Figure 15: Unweighted UniFrac PCoA plot showing the variation of the triweekly samples from the establishing biofilm. Each color represents one fraction. The upper right corner shows three distinct groupings: 1stFraction (red), 2nd Fraction (blue) and 3rd Fraction (yellow). The bottom left shows a spread grouping with a majority 4th Fraction (green) 5th Fraction (purple) and negative control (white).

3.10 Functional groups

3.10.1 Phosphorus accumulating organisms

The most prominent PAO is *Accumulibacter*, present at 0.7%, which represents 26.9% of all the PAOs in the establishing biofilm. The abundance of PAO's were not evenly distributed throughout the biofilm and as in the established biofilm the proportion of PAOs accumulated more deeper in the biofilm. Among the outer layer, with the most loosely associated bacteria, the average PAO proportion was 0.5% and peaked at 0.8% (Fig.16.d). It increased in the middle layer where the average was found to be 0.9% and the peak at 1.2%(Fig.16.e). Lastly, the inner layer had the highest abundance of PAOs with an average PAO proportion of 1.3% and a peak at 2.4% (Fig.16.f). Initially, the proportion PAO's increased in the entire biofilm, however, a considerable recession was observed from 15.03.17 to 05.04.17 throughout the biofilm(Fig.16.a-c). The recession of

PAO proportion affected the abundance more in the outer layer which was only present at 0.2% at the lowest trough (05.04.17), compared to 0.5% in the middle layer (21.04.17) and 0.6% in the inner layer (31.05.17). After the recession, an increase in PAO proportions was observed in all layers at 22.06.17, with the highest representation, by a small margin, was found in the inner layer at 1.3%, compared to 1.2% in the middle layer. The outer layer had 0.5% of PAOs at 22.06.17. The abundance of GAOs were proportional to the proportion of PAOs throughout the biofilm, however the presence of GAOs were consistently lower than the presence of PAOs through both the biofilm and over the entire studied time period. Only two genera of GAOs were identified, *Propionivibrio* and *Candidatus Competibacter*, where the former was found at a slightly higher proportion than the latter.

3.10.2 Other functional groups

As found in the established biofilm, denitrifiers decreased in abundance further into the establishing biofilm. The outer layer was found to have the highest average proportion of denitrifiers, at 25%, compared to the middle and inner layer which were found to have an average of 18% and 13%, respectively. In the 1st Fraction, *Hydrogenophaga* constituted 8.3% of the denitrifiers, while *Leucobacter* was the most represented genus, at 17.9%. Fermenters were the found to be the most abundant of the known functional group in both the middle and inner layers, where the middle layer had consistently larger proportion than the inner layer, except for 05.04.17. The two most prominent fermenters in the establishing biofilm was *Acetobacterium* and *Trichococcus* that made up 14.2% and 13.2% of the average proportion of fermenters, respectively. All fractions in the establishing biofilm had an increasing proportion of bacteria with unknown function, with the biggest increase observed in 1st Fraction, from 28% - 55% (Fig.16.a). The 3rd Fraction had the largest proportion of unknown bacteria at the end of the study, 63% (Fig.16.c). The group with unknown functions is a diverse group, including many sequences that were unidentifiable by the SILVA database. The two identifiable genera that was most abundant of the unknown bacteria was *Delftia*, at 4.1%, and *Chryseobacterium*, at 3.1%, or the average proportion in the establishing biofilm.

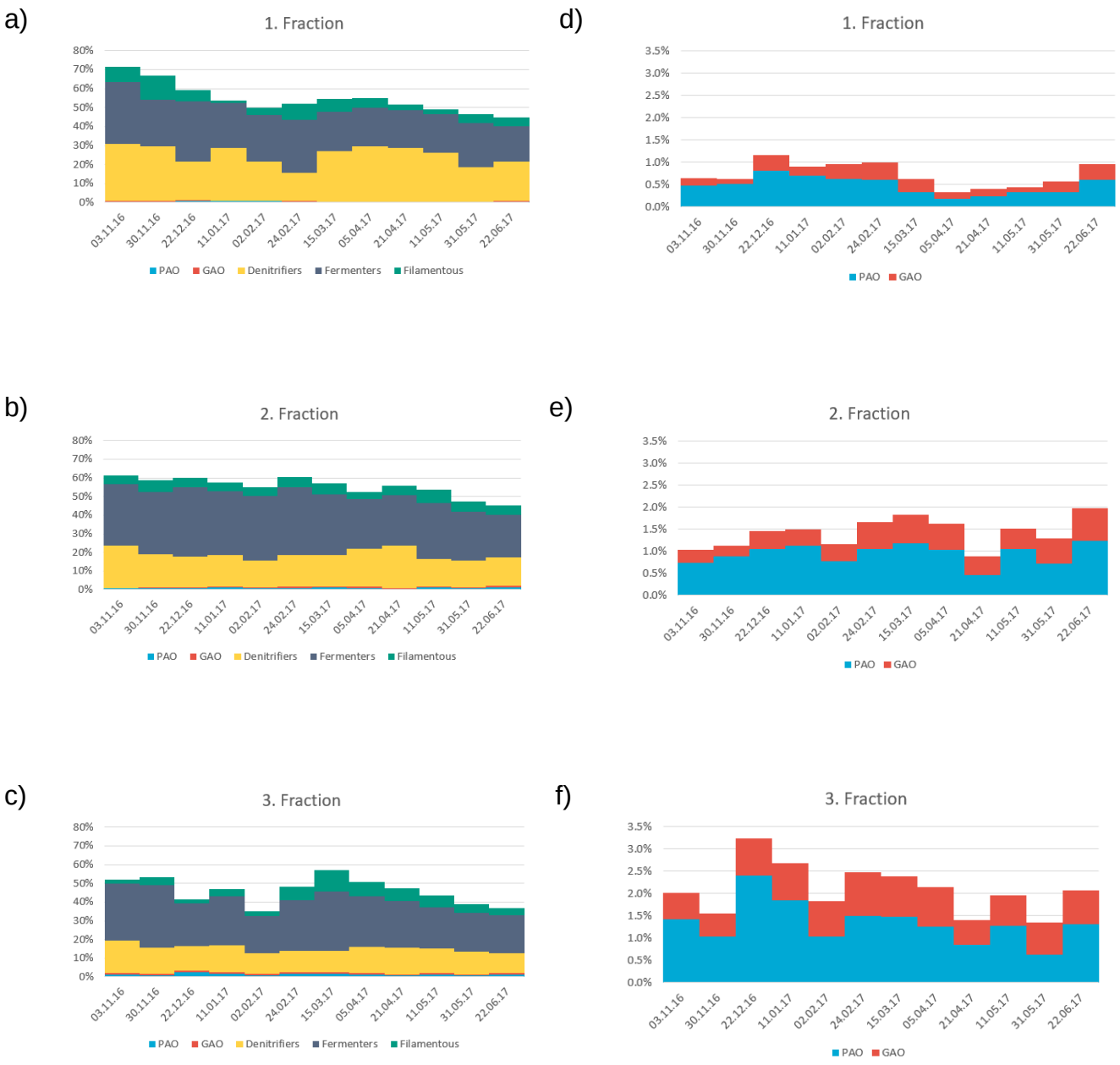

Figure 16: Functional groups in the establishing biofilm. Percentage of abundance of functional groups of bacteria from biofilms attached to biofilm carriers collected between 30.11.16 and 22.06.17. a-c) Shows the percentage of PAOs, GAOs, denitrifiers, fermenters and filamentous groups of bacteria over the studied time period in a) the outer layer b) the middle layer, and c) the inner layer of the establishing biofilm. d-f) Shows the cut out and magnified percentage of both PAOs and GAOs from the graphs a-c, over the studied time period in d) the outer layer, e) the middle layer, and f) the inner layer of the establishing biofilm.

Discussion

For a better understanding of the functional properties and interspecies interaction in biofilms, it is important to understand biofilm spatial composition. This understanding could benefit biological phosphorus removal in WWTP by yielding important insight to make phosphorus removal a source of recycled phosphorus in the future. In the present study, fractionation of the biofilm showed that the abundance of PAOs increase further into the biofilm, which differ from the theorized model, where PAO's were thought to accumulate most in the middle layer. The differences in composition between the establishing and the established biofilm, suggest that the biofilm takes much longer time to develop than previously thought (Goa, 2018).

4.1 Established biofilm

4.1.1 Quantity and diversity.

The fractionation of the samples from the established biofilm show a high similarity in taxonomy between each fraction from different samples (Fig.11), suggesting that the fractionation is successfully extracting the same fraction for each sample. This is further supported by the consistent copy number of 16S rRNA gene extracted from each fraction, shown by the low standard deviation, indicates that the consistent similarity in the diversity within each fraction is caused by the same amount of sequences, suggesting that each fractionation step extracts the same portion of the biofilm in every sample.

The only fraction that deviated from the others regarding varying copy number is the 4th fraction, where some samples differed from others in obtained copy number (Fig.9). Either way, given that no OTUs were observed from the fifth fractionation, it can be inferred that the 4th fraction constitutes the bacteria that was too tightly associated with the biofilm-carrier to be extracted by the third fractionation step. Furthermore, given the high degree

of overlap between the 3rd and the 4th fraction (Fig.11) it is practical to view them as two subdivisions of the inner layer, where the 3rd fraction constitutes the majority of the copy numbers (86%).

The largest fraction, the 2nd fraction, had both highest number of observed OTUs and the lowest beta-diversity, which indicates that there is high degree of overlap of OTUs in each sample. This suggests that the second fractionation step extracts the same portion of the biofilm in each sample. The same consistency is also observed in copy number of 16S rRNA gene, where a low variance is observed between the samples. The difference in diversity between the 1st and 2nd fraction coupled with the low of diversity within the 2nd fraction suggests that the same loosely associated layer of bacteria is extracted from each sample after the first fractionation, thus leaving each biofilm compositionally alike. If the starting point is the same for the second fractionation step in each sample, it follows that the portion size and the diversity is consistent in all samples, as observed. The 2nd fraction makes up the majority of the biofilm that form the middle layer of the biofilm. This leaves behind the remaining bacteria that was tightly associated with the biofilm demonstrated that the much smaller inner layer required five consecutive runs of the same fractionation program as the second fractionation with sand as scraping medium.

The biggest difference in diversity within a fraction was observed in the 1st Fraction (Fig.11). However, the variance between the samples from the 1st Fraction regarding copy number of 16S rRNA genes was not greater than the 2nd or the 3rd fraction, suggesting that the fractionation step is as consistent as the others. In addition, the low beta-diversity in the 2nd fraction indicate that if the first fractionation were to extract more the impact is probably minimal on the middle layer. As observed in the Unweighted UniFrac PCoA plot (Fig.11) the cluster for the 1st fraction had the largest distance from the other fractions, meaning that the fraction is compositionally the most different fraction. This fits the expectations of the outer layer of the biofilm.

4.1.2 Phosphorus Accumulating Organisms

The abundance of PAOs increased the further into the biofilm that were observed, not in the middle layer as previously assumed. This is observed all the way into the subdivisions of the inner layer, where nearly half of the bacteria tightest associated with the biofilm were PAOs (Fig.12). One explanation for this composition, as phosphorus removal average is 97%, could be that oxygen is able to penetrate far enough into the biofilm to reach the inner part, thus supplying the inner layer with the oxygen needed to accumulate Poly-P. However, the average phosphorus removal reached 95% even before 03.11.16(Goa, 2018) where the proportion of PAOs were 0.5%, 0.7% and 1.4% from outer to inner layer. Given that the observed proportion of PAOs where sufficient for the reported level of phosphorus removal it is likely that increasing the proportion increases stability, but it stills begs the question why the increase in the inner layer goes from 1.4% to 44.4% in two years. Alternatively, since anaerobic chambers with a high availability of easily degradable carbon was used to select for PAOs, the same environment can be created within the biofilm, by fermenters producing the necessary carbon sources (Nielsen et al., 2010). Studies exploring the distribution of accumulated Poly-P, may give crucial insight into the spatial composition of PAOs in the established, as well as the establishing biofilm.

4.1.3 Glucose Accumulating Organisms

The same spatial composition found in PAOs, growing in abundance further into the biofilm, was found in GAOs. However, at much lower abundance at 1.6%, 2.0% and 2.3% from outer to inner layer. The PAO to GAO ratio is considerably lower in the established biofilm than in the establishing biofilm. This comparative reduction suggests that the GAOs function in the biofilm diminishes, which is reflected in the increase in phosphorus uptake. It is clear the GAOs are losing the competition for the VFA against the PAOs. Whether this is caused by a biofilm saturated with oxygen, letting the PAOs accumulate

Poly-P or other factor cannot be stated at this point in time, but studies examining the distribution of Poly-P through the biofilm could potentially shed some light over this question.

4.1.4 Denitrifiers

In contrast with PAOs the abundance of denitrifiers diminishes towards the inner layer, where the group made up the largest functional group on the outer layer. The average proportion of denitrifiers found in the established biofilm matches the proportion found in the Danish study, at 18% (Nielsen et al., 2010). Previous studies have shown that denitrification during anaerobic phase can cause competition for the PAOs (Baetens, 2001), given that many denitrifiers also consume acetate and other VFA. On the other hand, no nitrifiers were obtained from HIAS WWTP, whereas the Danish study (Nielsen et al., 2010) had an average proportion of 7%, thus it is reasonable to assume there is a significant difference in nitrate produced. Had nitrate been present, the pilot study at HIAS showed that the plant has potential for SND (Saltnes et al., 2017) and if excess nitrate had been left over at the end of the plant, the biofilm-carriers are moved without it the sewage water. It is therefore reasonable to believe that the denitrifiers do not hinder phosphate accumulation in the established plant. Studies have shown that some denitrifiers have a broader spectrum of potential carbon sources in aerobic environments than in anaerobic conditions (Balch et al., 1977). This might be part in explaining why *Hydrogenophaga* is the most abundant genus in the outer layer, where it is most exposed to oxygen, as *Hydrogenophaga* is a hydrogen-oxidizing bacterium (Willems et al., 1989).

4.1.5 Fermenters

The average proportions of fermenters were found to be over three times that of the average proportion in the Danish study, at 9.4% and 3% respectively (Nielsen et al., 2010). This discrepancy could potentially be caused by a difference of oxygen penetration through the biofilm growth on biofilm-carrier compared to that of the flocs in the classic EBPR plants, however no studies have been conducted on the topic. Given that the middle layer is the richest in fermenters, there are at least enclaves in the biofilm that are

not exposed to oxygen. The most abundant genus in the middle layer, *Proteiniclastiucum* of the phylum *Firmicutes*, can ferment glucose to VFAs such as acetate (Nielsen et al., 2010). This suggests that the model created at HIAS (Fig.5) which shows the fermenters produce VFA in the inner layer and transferring it towards the middle layer is in reality the other way around. In addition, under anaerobic conditions, fermentative bacteria can produce hydrogen gas through a process called dark hydrogen fermentation (Nath et al., 2004). It is possible that this hydrogen gas is produced in the middle layer and dissipates out to the outer layer creating conditions that select for the high abundance of *Hydrogenophaga* in the outer layer.

4.1.6 Bacteria with unknown function

In Danish study, 10-20% of the entire community was bacteria with a unknown function, which is at the most only half of that found in the established biofilm. It is hard to assess what the actual differences are between the biofilms studied and what is the cause of difference in method for identifying functional groups. *Desulfobulbus*, being one of the most abundant genera in the established biofilm, is sulphate reducer (Pagani et al., 2011), a functional group not accounted for in this study. Further studies into Sulphur metabolism could help shed light on parts of the mysteries hidden in the unknown group.

4.2 Establishing biofilm

4.2.1 Quantity and diversity

Since the 4th fraction had a high degree of overlap with the general cluster of the 5th fraction and the negative controls (Fig.15), as well as all three showing similarly low levels of observed OTUs. It is reasonable to assume that the third fractionation step extracted all the detectable bacteria associated with the biofilm. A potential explanation for why this occurred in the establishing biofilm and not the established biofilm is that the established biofilm is thicker than the establishing biofilm. This hypothesis could be explored by analyzing the biofilms under an electron microscope to measure thickness, or by drying the biofilms and weighing the dry biomass. Both methods would give valuable information about the physical size of the biofilm in relation to the spatial composition.

The first fractionation step did not extract a consistent copy number of the 16S rRNA gene across over time (Fig.13). This further supports the notion that the first fractionation step extracts bacteria loosely associated on the outer layer of the biofilm and reaches a "threshold" regarding adhesion to the biofilm matrix, as opposed to extracting an equal outer portion of the biofilm. With the loosely associated bacteria extracted, the second fractionation step presumably has a similar starting point upon extraction in each sample across time. This is mirrored in the consistency found in copy number over the studied time period. Corresponding well with the middle layer of the established biofilm, the copy number of the 2nd fraction was on average the highest in the establishing biofilm. Given the consistency of the 2nd fraction, the variation observed in copy number of the 3rd fraction is most likely caused by difference in thickness of the biofilm over time.

Both the outer and inner layer shows a spike in copy number at in the same time span (24.02.17 to 05.04.17) (Fig.13). The study at HIAS WWTP showed that the composition of the wastewater changes, not only month by month, by also day by day. These are variables not controlled for in this study, which makes it impossible to assess the cause of this change in the biofilm. One could speculate that the spike occurs in the spring, when snow melts, increasing the water content as well as lowering the temperature, both factors shown to affect the biofilm composition (Nielsen et al., 2010).

The number of observed OTUs follows the same trend in the establishing biofilm as in the established, the middle being the richest, followed by the inner layer and lastly the outer layer (Fig.14). However, while the three layers form individual clusters, the difference in diversity between layers is lower in the establishing biofilm, indicating that as the biofilm matures it differentiates more in spatial composition.

4.2.1 Phosphorus Accumulating Organisms

The average proportion of PAOs over time in the establishing biofilm is 0.9% compared to 33.6% in the established biofilm. Still, the phosphorus removal was on average ~95% (Goa, 2018), suggesting that the Poly-P uptake per cell is much higher in the establishing plant. It could also be other unknown PAOs contributing to phosphorus removal. The discrepancy in *Accumulibacter* representation between the establishing and the established biofilm, suggest that *Accumulibacter* is selected for in the WWTP. This is also observed in the Danish study where *Accumulibacter* is the most abundant. This can be caused by the PHA-storing ability of *Accumulibacter*, which is not shared by *Tetrasphaera*. The general trend regarding distribution of PAOs among the layers of the biofilm found in the established biofilm holds true during the development as well. However, the difference between the middle and inner layer is small, and the differentiation observed in the matured biofilm happens at a later point in time than the studied time period.

While the general trend observed is an increase in PAO abundance, a recession that coincides with the spike in amount of extracted DNA. The inner layer is the least affected, supporting the explanation that this is caused by environmental factors, as it would be the least exposed to the environment.

4.2.3 Glucose Accumulating Organisms

The average proportion of GAOs was 0.5%, which is lower than what was found in the Danish study (Nielsen et al., 2010), however, the PAO to GAO ratio is much lower. The high phosphorus removal indicates that the low ratio is not detrimental to the plants general function, which could happen if sufficient VFAs were present in the plant, so that the GAOs could not out-competing the PAOs.

4.2.4 Denitrifiers

The denitrifiers is the only functional group that was found to have a consistent average proportion in both the establishing and established biofilm, furthermore the Danish study found the same average, 18% (Nielsen et al., 2010). This does not mean that the distribution was the same. The outer layer had a higher diversity in the establishing plant, as well as *Leucobacter*, not *Hydrogenophaga* being the most represented genus. Neither of these were found to be the most common denitrifiers according to the Danish study. Since *Leucobacter* doesn't have oxidase (Tacheuchi 1992), it might be access to oxygen that favors *Hydrogenophaga*, but further studies are needed.

4.2.5 Fermenters

At an average proportion of 27.5%, fermenters were found at a considerably higher abundance in the establishing, than the established biofilm. It is reasonable to conclude that the higher proportion of fermenters results in a higher proportional amount of VFAs, as suggested above (See 4.2.3). This is further supported by the most abundant genus among the fermenters, *Acetobacterium,* which oxidizes hydrogen gas to produce acetate. Furthermore, with the abundance of hydrogen-oxidizers, it is plausible that the biofilm produces a large amount of hydrogen gas, which could explain how *Hydrogenophaga* is selected for.

4.2.6 Technical Issues and Limitations

While the biofilm-carriers are all uniformly produced, it seems that deformities can occur in the WWTP. These deformities did at times cause the biofilm-carriers to get stuck in the tubes during fractionation. Removing stuck biofilm-carriers can potentially cause mechanical stress not accounted for in the analysis. For example, the inconsistencies observed in copy number of 16S rRNA gene in the 4th fraction from the established biofilm could be a result of additional stress.

The establishing biofilms had been thawed and refrozen for a previous study, it is a possibility that this has interfered with

The first fractionation step was performed manually on a vortex mixer. Human error could potentially result in a harsher treatment than wanted. Thus, extracting more of the biofilm than the intended loosely associated bacteria on the outside, accounting for part of the internal difference in diversity of said fraction.

A limitation of the present study is that all information on the composition is inferred form the metagenomic data sets. The resulting fractions has not been observed to physically which could give a more definite answer on how the biofilm is physically altered.

Conclusion.

In the theorized model for spatial composition of the biofilms at HIAS continuous biofilm process plant it was assumed that the highest abundance of PAOs would occur in the middle layer. The present study has shown that the abundance of PAOs increases towards the inner layer of the biofilm. Considering the current findings, the theorized model needs to be revised.

The early onset of high (95%) phosphorus removal observed in at HIAS WWTP given the low abundance of PAOs (0.9%) during development, shows that functional development occurs much earlier than biofilm maturation. The large difference in abundance of PAOs between the biofilm during development (0.9%) and the matured biofilm (33.6%) that the compositional development of the biofilm is a much longer than phosphorus removal numbers would suggest.

It seems like the mechanical stress-based method utilized to fractionate the biofilms in the present study is a viable method, as it produced layers with distinct compositional and functional differences.

Referances

Baetens, D. (2001). *Enhanced biological phosphorus removal: modelling and experimental design*.

Balch, W. E., Schoberth, S., Tanner, R. S., Wolfe, R. J. I. J. o. S. & Microbiology, E. (1977). Acetobacterium, a new genus of hydrogen-oxidizing, carbon dioxide-reducing, anaerobic bacteria. 27 (4): 355-361.

Chmielewski, R., Frank, J. J. C. r. i. f. s. & safety, f. (2003). Biofilm formation and control in food processing facilities. 2 (1): 22-32.

Cordell, D., Rosemarin, A., Schröder, J. J. & Smit, A. J. C. (2011). Towards global phosphorus security: A systems framework for phosphorus recovery and reuse options. 84 (6): 747-758.

De-Bashan, L. E. & Bashan, Y. J. W. r. (2004). Recent advances in removing phosphorus from wastewater and its future use as fertilizer (1997–2003). 38 (19): 4222-4246.

Flemming, H.-C., Wingender, J., Szewzyk, U., Steinberg, P., Rice, S. A. & Kjelleberg, S. J. N. R. M. (2016). Biofilms: an emergent form of bacterial life. 14 (9): 563.

Gernaey, K. V., van Loosdrecht, M. C., Henze, M., Lind, M., Jørgensen, S. B. J. E. M. & Software. (2004). Activated sludge wastewater treatment plant modelling and simulation: state of the art. 19 (9): 763-783.

Goa, I. A. N. (2018). *Characterization of the Microbiota Composition Associated with the Hias Continuous Biofilm Process*. Masteroppgave. Ås: Norges miljø- og biovitenskapelige universitet. Available at: https://nmbu.brage.unit.no/nmbu-xmlui/bitstream/handle/11250/2566155/Goa2018.pdf?sequence=1&isAllowed=y (accessed: 09.08.2018).

Jasinski, S. M. (2018). *Phosphate rock*. Mineral Commodity Summaries. Available at: https://prd-wret.s3-us-west-2.amazonaws.com/assets/palladium/production/atoms/files/mcs-2019-phosp.pdf (accessed: 05.04.2019).

Kok, D.-J. D., Pande, S., Lier, J. B. v., Ortigara, A. R., Savenije, H., Uhlenbrook, S. J. H. & Sciences, E. S. (2018). Global phosphorus recovery from wastewater for agricultural reuse. 22 (11): 5781-5799.

Lappin-Scott, H., Burton, S. & Stoodley, P. J. N. R. M. (2014). Revealing a world of biofilms—the pioneering research of Bill Costerton. 12 (11): 781.

Løvik, J. E. R., Sigurd

Fjeld, Erik

Kjellberg, Gösta (2009). *Mjøsa*.

Mahami, T. & Adu-Gyamfi, A. J. I. R. J. M. (2011). Biofilm-associated infections: public health implications. 2 (10): 375-381.

Nath, K., Das, D. J. A. m. & biotechnology. (2004). Improvement of fermentative hydrogen production: various approaches. 65 (5): 520-529.

Nielsen, P. H., Mielczarek, A. T., Kragelund, C., Nielsen, J. L., Saunders, A. M., Kong, Y., Hansen, A. A. & Vollertsen, J. J. W. r. (2010). A conceptual ecosystem model of microbial communities in enhanced biological phosphorus removal plants. 44 (17): 5070-5088.

O'Toole, G., Kaplan, H. B. & Kolter, R. J. A. R. i. M. (2000). Biofilm formation as microbial development. 54 (1): 49-79.

Padedda, B. M., Sechi, N., Lai, G. G., Mariani, M. A., Pulina, S., Sarria, M., Satta, C. T., Virdis, T., Buscarinu, P., Lugliè, A. J. G. E., et al. (2017). Consequences of eutrophication in the management of water resources in Mediterranean reservoirs: A case study of Lake Cedrino (Sardinia, Italy). 12: 21-35.

Pagani, I., Lapidus, A., Nolan, M., Lucas, S., Hammon, N., Deshpande, S., Cheng, J.-F., Chertkov, O., Davenport, K. & Tapia, R. J. S. i. g. s. (2011). Complete genome sequence of Desulfobulbus propionicus type strain (1pr3 T). 4 (1): 100.

Rybicki, S. M. (1998). *New technologies of phosphorus removal from wastewater*. Proc. Of a Polish-Swedish Seminar, Joint Polish Swedish Reports, Report.

Saltnes, T., Sørensen, G., Eikås, S. J. W. P. & Technology. (2017). Biological nutrient removal in a continuous biofilm process. 12 (4): 797-805.

Seviour, R. J., Mino, T. & Onuki, M. J. F. m. r. (2003). The microbiology of biological phosphorus removal in activated sludge systems. 27 (1): 99-127.

Sverdrup, H. U. & Ragnarsdottir, K. V. J. A. G. (2011). Challenging the planetary boundaries II: Assessing the sustainable global population and phosphate supply, using a systems dynamics assessment model. 26: S307-S310.

Tarayre, C., Nguyen, H.-T., Brognaux, A., Delepierre, A., De Clercq, L., Charlier, R., Michels, E., Meers, E. & Delvigne, F. J. S. (2016). Characterisation of phosphate accumulating organisms and techniques for polyphosphate detection: a review. 16 (6): 797.

Willems, A., Busse, J., Goor, M., Pot, B., Falsen, E., Jantzen, E., Hoste, B., Gillis, M., Kersters, K., Auling, G. J. I. J. o. S., et al. (1989). Hydrogenophaga, a new genus of hydrogen-oxidizing bacteria that includes Hydrogenophaga flava comb. nov.(formerly Pseudomonas flava), Hydrogenophaga palleronii (formerly Pseudomonas palleronii), Hydrogenophaga pseudoflava (formerly Pseudomonas pseudoflava and “Pseudomonas carboxydoflava”), and Hydrogenophaga taeniospiralis (formerly Pseudomonas taeniospiralis). 39 (3): 319-333.

WWF. (u.å.). Kaldnes® MBBR.

Yang, K., Li, Z., Zhang, H., Qian, J. & Chen, G. J. E. t. (2010). Municipal wastewater phosphorus removal by coagulation. 31 (6): 601-609.

Appendix

Appendix A: PCR Reagents with Function

Table A1. The reagents used for first stage PCR and the function of them. (Goa, 2018)

Reagents:	**Function:**
5 x HOT FIREPol® Blend Master Mix Ready to Load:	
5 x HOT FIREPol® DNA polymerase	A warm stable enzyme that synthesize the complementary DNA strand in the 5`→3`direction
Proofreading enzyme	Error correcting enzyme that has both the 5`→3`exonuclease activity in addition to 3`→5 proofreading activity
5 x Blend Master Mix Buffer	Optimize the conditions for "5 x HOT FIREPol® Blend Master Mix Ready to Load". Including it facilitates the primer binding
12,5 mM $MgCl_2$ 1 x PCR solution – 1,5 mM $MgCl_2$	Required for primer binding, T_m of template DNA and function as a cofactor for DNA polymerase
2 mM dNTPs of each 1 x PCR solution 200 µM dATP, 200 µM dCTP, 200 µM dGTP and 200 µM dTTP	Nucleotides which the DNA polymerase use as building blocks to synthesize the complementary DNA strand.
Bovine Serum Albumin (BSA)	BSA increases PCR yields from low purity templates. It also prevents adhesion of enzymes to the reaction tubes and tip surface.
Blue dye migration equivalent to 3,5-4,5 kb DNA fragment **Yellow dye** migration rat in excess of primers in 1% agarose gel: <35-45bp	Compounds that makes it possible to directly load the samples onto agarose gel and to track the dyes during the electrophoresis
Unknown compound	Compound that increases sample density for direct loading
Forward primer - 16S rRNA gene **Reverse primer - 16S rRNA gene**	The universal prokaryote primers PRK341F and PRK806R was used for amplification of the variable regions, V3 and V4, of the 16S gene. The 3`end of these primers are designed to bind to the 16S gene.

Forward primer – 18S rRNA gene **Reverse primer - 18S rRNA gene**	The PCR primers 3NDF[1] and V4_Euk_R2[2] target a 450bp region that encompass the variable V4 of the 18S rRNA gene. The 3`end of these primers are designed to bind to the 18S gene.
Nuclease-free water	Used to dilute the concentration of the other reagents to the proper final concentration. In addition it helps to avoid DNA degradation by nucleases as well as interference of the PCR reaction by ions which could be present in otherwise not nuclease free deionized water.
DNA template	DNA isolated from biofilms collected at wastewater treatment plants in Hamar

Table A2. The reagents used for index PCR and the function of them. (Goa, 2018)

Reagents:	**Function:**
5 x FIREPol® Master Mix Ready to Load:	
FIREPol® DNA polymerase	A warm stable enzyme that synthesize the complementary DNA strand in the 5`→3`direction
5 x Reaction Buffer	Optimize the conditions for "5 x HOT FIREPol® Blend Master Mix Ready to Load". Including it facilitates the primer binding
12,5 mM $MgCl_2$ 1 x PCR solution – 1,5 mM $MgCl_2$	Required for primer binding, T_m of template DNA and function as a cofactor for DNA polymerase
1 mM dNTPs of each 1 x PCR solution 200 µM dATP, 200 µM dCTP, 200 µM dGTP and 200 µM dTTP	Nucleotides which the DNA polymerase use as building blocks to synthesize DNA strands
Blue dye migration equivalent to 3,5-4,5 kb DNA fragment **Yellow dye** migration rat in excess of primers in 1% agarose gel: <35-45bp	Compounds that makes it possible to directly load the samples onto agarose gel and to track the dyes during the electrophoresis
Unknown compound	Compound that increases sample density for direct loading
Forward index primer – rRNA 16S gene **Reverse index primer – rRNA 16S gene**	The universal prokaryote primers PRK341F and PRK806R was used for amplification of the variable regions, V3 and V4, of the 16S gene. The 3`end of these primers are designed to bind to the 16S gene. The 5`end of the primers are modified with an adaptor sequence which is complementary to oligonucleotide

	sequences on the flow cell surface of the Illumina sequence platform
Forward index primer – 18S rRNA gene **Reverse index primer – 18S rRNA gene**	– The PCR primers, 3NDF[1] and V4_Euk_R2[2], target a 450bp region that encompass the variable V4 of the 18S rDNA gene. The 3`end of these primers are designed to bind to the 18S gene. The 5`end of the primers are modified with an adaptor sequence which is complementary to oligonucleotide sequences on the flow cell surface of the Illumina sequence platform
Nuclease-free water	Used to dilute the concentration of the other reagents to the proper final concentration. In addition it helps to avoid DNA degradation by nucleases as well as interference of the PCR reaction by ions which could be present in otherwise not nuclease free deionized water.
DNA template	DNA isolated from biofilms collected at wastewater treatment plants in Hamar

Tabell A3. The reagents used for qPCR and the function of them (Goa, 2018)

Reagents	**Purpose**
5x HOT FIREPol® **EvaGreen® qPCR supermix**:	
HOT FIREPol DNA Polymerase	A warm stable enzyme that synthesize the complementary DNA strand in the 5`→3`direction
5x EvaGreen qPCR buffer	Optimize the conditions for reagensene in the "5x HOT FIREPol® EvaGreen® qPCR supermix". Including it facilitates the primer binding
12,5 mM $MgCl_2$ 1x PCR solution – 2,5 mM	Required for primer binding, T_m of template DNA and function as a cofactor for DNA polymerase
dNTPs	Nucleotides which the DNA polymerase use as building blocks to synthesize DNA strands
EvaGreen dye	EvaGreen® dye is a green fluorescent nucleic acid dye. The dye is essentially nonfluorescent by itself but becomes highly fluorescent upon binding to dsDNA.
Internal reference based on ROX dye	ROX is an internal passive reference dye used to normalize the fluorescent reporter signal generated in qPCR
GC-rich Enhancer	The purpose of the GC-rich enhancer is to bring the melting temperature of GC rich regions closer into line with AT regions so that the primers anneal quickly and uniformly.
Blue visualization dye	Used for loading and visualize the PCR products on agarose gel
Forward primer - 16S rRNA gene **Reverse primer - 16S rRNA gene**	The universal prokaryote primers PRK341F and PRK806R was used for amplification of the variable regions, V3 and V4, of the 16S gene. The 3`end of these primers are designed to bind to the 16S gene.
Forward primer – 18S rRNA gene **Reverse primer - 18S rRNA gene**	The PCR primers 3NDF[1] and V4_Euk_R2[2] target a 450bp region that encompass the variable V4 of the 18S rRNA gene. The 3`end of these primers are designed to bind to the 18S gene.

Nuclease-free water	Used to dilute the concentration of the other reagents to the proper final concentration. In addition, it helps to avoid DNA degradation by nucleases as well as interference of the PCR reaction by ions which could be present in otherwise not nuclease free deionized water.
Template DNA	DNA isolated from biofilms collected at wastewater treatment plants in Hamar

Appendix B: PRK Illumina Primers

Table B.1. Properties of 341F and 806R primers for PCR. (Goa, 2018)

Primer name	Primer sequence 5`-->3`	Target gene	Gene length	Annealing temp (˚C)	References
PRK341F	CCTACGGGRBGCASCAG	V3-V4 region of 16S rRNA	466	55	Yu et al. 2005
PRK806R	GGACTACYVGGGTATCTAAT	V3-V4 region of 16S rRNA	466	55	Yu et al. 2005

Table B.2. Illumina primers (Goa, 2018)

PRK Illumina forward primers (5' - 3'):

1. aatgatacggcgaccaccgagatct acactctttccctacacgacgctcttccgatctagtcaa CCTACGGGRBGCASCAG
2. aatgatacggcgaccaccgagatct acactctttccctacacgacgctcttccgatctagttcc CCTACGGGRBGCASCAG
3. aatgatacggcgaccaccgagatct acactctttccctacacgacgctcttccgatctatgtca CCTACGGGRBGCASCAG
4. aatgatacggcgaccaccgagatct acactctttccctacacgacgctcttccgatctccgtcc CCTACGGGRBGCASCAG
5. aatgatacggcgaccaccgagatct acactctttccctacacgacgctcttccgatctgtagag CCTACGGGRBGCASCAG
6. aatgatacggcgaccaccgagatct acactctttccctacacgacgctcttccgatctgtccgc CCTACGGGRBGCASCAG
7. aatgatacggcgaccaccgagatct acactctttccctacacgacgctcttccgatctgtgaaa CCTACGGGRBGCASCAG
8. aatgatacggcgaccaccgagatct acactctttccctacacgacgctcttccgatctgtggcc CCTACGGGRBGCASCAG
9. aatgatacggcgaccaccgagatct acactctttccctacacgacgctcttccgatctgtttcg CCTACGGGRBGCASCAG
10. aatgatacggcgaccaccgagatct acactctttccctacacgacgctcttccgatctcgtacg CCTACGGGRBGCASCAG
11. aatgatacggcgaccaccgagatct acactctttccctacacgacgctcttccgatctgagtgg CCTACGGGRBGCASCAG

12. aatgatacggcgaccaccgagatct acactctttccctacacgacgctcttccgatctggtagc CCTACGGGRBGCASCAG

13. aatgatacggcgaccaccgagatct acactctttccctacacgacgctcttccgatctactgat CCTACGGGRBGCASCAG

14. aatgatacggcgaccaccgagatct acactctttccctacacgacgctcttccgatctatgagc CCTACGGGRBGCASCAG

15. aatgatacggcgaccaccgagatct acactctttccctacacgacgctcttccgatctattcct CCTACGGGRBGCASCAG

16. aatgatacggcgaccaccgagatct acactctttccctacacgacgctcttccgatctcaaaag CCTACGGGRBGCASCAG

PRK Illumina reverse primers (5' - 3'):

1. caagcagaagacggcatacgagatcgtgat gtgactggagttcagacgtgtgctcttccgatctGGACTACYVGGGTATCTAAT

2. caagcagaagacggcatacgagatacatcg gtgactggagttcagacgtgtgctcttccgatctGGACTACYVGGGTATCTAAT

3. caagcagaagacggcatacgagatgcctaa gtgactggagttcagacgtgtgctcttccgatctGGACTACYVGGGTATCTAAT

4. caagcagaagacggcatacgagattggtca gtgactggagttcagacgtgtgctcttccgatctGGACTACYVGGGTATCTAAT

5. caagcagaagacggcatacgagatcactct gtgactggagttcagacgtgtgctcttccgatctGGACTACYVGGGTATCTAAT

6. caagcagaagacggcatacgagatattggc gtgactggagttcagacgtgtgctcttccgatctGGACTACYVGGGTATCTAAT

7. caagcagaagacggcatacgagatgatctg gtgactggagttcagacgtgtgctcttccgatctGGACTACYVGGGTATCTAAT

8. caagcagaagacggcatacgagattcaagt gtgactggagttcagacgtgtgctcttccgatctGGACTACYVGGGTATCTAAT

9. caagcagaagacggcatacgagatctgatc gtgactggagttcagacgtgtgctcttccgatctGGACTACYVGGGTATCTAAT

10. caagcagaagacggcatacgagataagcta gtgactggagttcagacgtgtgctcttccgatctGGACTACYVGGGTATCTAAT

11. caagcagaagacggcatacgagatgtagcc gtgactggagttcagacgtgtgctcttccgatctGGACTACYVGGGTATCTAAT

12. caagcagaagacggcatacgagattacaag gtgactggagttcagacgtgtgctcttccgatctGGACTACYVGGGTATCTAAT

13. caagcagaagacggcatacgagatttgact gtgactggagttcagacgtgtgctcttccgatctGGACTACYVGGGTATCTAAT

14. caagcagaagacggcatacgagatggaact gtgactggagttcagacgtgtgctcttccgatctGGACTACYVGGGTATCTAAT

15. caagcagaagacggcatacgagattgacat gtgactggagttcagacgtgtgctcttccgatctGGACTACYVGGGTATCTAAT

16. caagcagaagacggcatacgagatggacgg gtgactggagttcagacgtgtgctcttccgatctGGACTACYVGGGTATCTAAT

17. caagcagaagacggcatacgagatctctac gtgactggagttcagacgtgtgctcttccgatctGGACTACYVGGGTATCTAAT

18. caagcagaagacggcatacgagatgcggac gtgactggagttcagacgtgtgctcttccgatctGGACTACYVGGGTATCTAAT

19. caagcagaagacggcatacgagattttcac gtgactggagttcagacgtgtgctcttccgatctGGACTACYVGGGTATCTAAT

20. caagcagaagacggcatacgagatggccac gtgactggagttcagacgtgtgctcttccgatctGGACTACYVGGGTATCTAAT

21. caagcagaagacggcatacgagatcgaaac gtgactggagttcagacgtgtgctcttccgatctGGACTACYVGGGTATCTAAT

22. caagcagaagacggcatacgagatcgtacg gtgactggagttcagacgtgtgctcttccgatctGGACTACYVGGGTATCTAAT

23. caagcagaagacggcatacgagatccactc gtgactggagttcagacgtgtgctcttccgatctGGACTACYVGGGTATCTAAT

24. caagcagaagacggcatacgagatgctacc gtgactggagttcagacgtgtgctcttccgatctGGACTACYVGGGTATCTAAT

25. caagcagaagacggcatacgagatatcagt gtgactggagttcagacgtgtgctcttccgatctGGACTACYVGGGTATCTAAT

26. caagcagaagacggcatacgagatgctcat gtgactggagttcagacgtgtgctcttccgatctGGACTACYVGGGTATCTAAT

27. caagcagaagacggcatacgagataggaat gtgactggagttcagacgtgtgctcttccgatctGGACTACYVGGGTATCTAAT

28. caagcagaagacggcatacgagatcttttg gtgactggagttcagacgtgtgctcttccgatctGGACTACYVGGGTATCTAAT

29. caagcagaagacggcatacgagattagttg gtgactggagttcagacgtgtgctcttccgatctGGACTACYVGGGTATCTAAT

30. caagcagaagacggcatacgagatccggtg gtgactggagttcagacgtgtgctcttccgatctGGACTACYVGGGTATCTAAT

31. caagcagaagacggcatacgagatatcgtg gtgactggagttcagacgtgtgctcttccgatctGGACTACYVGGGTATCTAAT

32. caagcagaagacggcatacgagattgagtg gtgactggagttcagacgtgtgctcttccgatctGGACTACYVGGGTATCTAAT

33. caagcagaagacggcatacgagatcgcctg gtgactggagttcagacgtgtgctcttccgatctGGACTACYVGGGTATCTAAT

34. caagcagaagacggcatacgagatgccatg gtgactggagttcagacgtgtgctcttccgatctGGACTACYVGGGTATCTAAT

35. caagcagaagacggcatacgagataaaatg gtgactggagttcagacgtgtgctcttccgatctGGACTACYVGGGTATCTAAT

36. caagcagaagacggcatacgagattgttgg gtgactggagttcagacgtgtgctcttccgatctGGACTACYVGGGTATCTAAT

Appendix: C

Table of functional groups from received from HIAS WWTP

Pao
- Tetrasphaera
- Accumulibacter

GAO
- Competibacter
- Propionivibrio
- Spb280

Nitrifiers AOB
- Nitrosimans

NOB
- Nitrotoga
- Nitrospira

Denitrifirs
- Pseudorhodobacter
- Acidovorax
- Hydrogenophaga
- Rhodoferax
- Simplicispira
- Flavobacterium
- Laucobacter
- Comamonas

Fermentering
- Clostridia
- Paludibacter
- Tetrasphera
- Trichococcus
- Streptococcus
- Vacococcus
- Lactococcus
- Lauctococcus
- Propionivibrio
- Flavobacterium
- Rhodoferax

Filiamentous
- Chloroflexi
- Microthrix
- Trichococcus

Norges miljø- og biovitenskapelige universitet
Noregs miljø- og biovitskapelege universitet
Norwegian University of Life Sciences

Postboks 5003
NO-1432 Ås
Norway